ผลกระทบของอัตราการเฉือนต่อความแข็งและความเหนียว
ของรอยแตกในหินทราย

นายฮาซัน คอแด๊ะ

วิทยานิพนธ์นี้เป็นส่วนหนึ่งของการศึกษาตามหลักสูตรปริญญาวิศวกรรมศาสตรมหาบัณฑิต
สาขาวิชาเทคโนโลยีธรณี
มหาวิทยาลัยเทคโนโลยีสุรนารี
ปีการศึกษา 2556

EFFECT OF SHEAR RATE ON STRENGTH AND STIFFNESS OF SANDSTONE FRACTURES

Hasun Kodae

A Thesis Submitted in Partial Fulfillment of the Requirements for the Degree of Master of Engineering in Geotechonolgy

Suranaree University of Technology

Academic Year 2013

EFFECT OF SHEAR RATE ON STRENGTH AND STIFFNESS OF SANDSTONE FRACTURES

Suranaree University of Technology has approved this thesis submitted in partial fulfillment of the requirements for a Master's Degree.

Thesis Examining Committee

____

(Dr. Prachya Tepnarong)

Chairperson

____

(Prof. Dr. Kittitep Fuenkajorn)

Member (Thesis Advisor)

____

(Dr. Decho Phueakphum)

Member

______________________________	______________________________
(Prof. Dr. Sukit Limpijumnong)	(Assoc. Prof. Flt. Lt. Dr. Kontorn Chamniprasart)
Vice Rector for Academic Affairs and Innovation.	Dean of Institute of Engineering

ฮาซัน คอแด๊ะ : ผลกระทบของอัตราการเฉือนต่อความแข็งและความเหนียวของรอยแตกในหินทราย (EFFECT OF SHEAR RATE ON STRENGTH AND STIFFNESS OF SANDSTONE FRACTURES) อาจารย์ที่ปรึกษา : ศาสตราจารย์ ดร.กิตติเทพ เฟื่องขจร, 58 หน้า.

วัตถุประสงค์ของงานวิจัยนี้คือเพื่อศึกษาผลกระทบของอัตราการให้แรงเฉือนต่อค่ากำลังเฉือนและค่าความเหนียวของรอยแตกในหินทราย โดยหินทรายที่ใช้ในการทดสอบเป็นหินจากชุดหินทรายพระวิหาร ภูกระดึง และภูพาน รอยแตกของตัวอย่างหินทำขึ้นในห้องปฏิบัติการโดยวิธีการให้แรงกดแบบแนวเส้นเพื่อให้เกิดแรงดึงในตัวอย่างหิน พื้นที่หน้าตัดของรอยแตกที่ใช้ในการทดสอบมีขนาด 90×100 ตารางมิลลิเมตร โดยให้แรงกดตั้งฉากกับรอยแตกคงที่ผันแปรจาก 1, 2, 3 ถึง 4 เมกกะปาสคาล และใช้อัตราการเฉือนผันแปรจาก 10^{-4} ถึง 10^{-1} มิลลิเมตรต่อวินาที ผลการวิจัยที่ได้สำหรับหินทรายทั้งหมดที่ใช้ในการทดสอบพบว่า ค่ากำลังรับแรงเฉือนสูงสุด ค่ากำลังรับแรงเฉือนคงเหลือและค่าความเหนียวของรอยแตกเพิ่มขึ้นแบบเอกซ์โพเนนเชียลกับอัตราการให้แรง โดยเฉพาะอย่างยิ่งภายใต้สภาวะความเค้นกดตั้งฉากสูง อัตราการเฉือนจะไม่มีผลกระทบกับมุมเสียดทานพื้นฐานของรอยแตกที่มีพื้นผิวเรียบ พื้นฐานเกณฑ์การแตกของคูร์ลอมบ์ค่าความเค้นยึดติดจะมีค่าเข้าใกล้ศูนย์ที่อัตราการเฉือนเท่ากับ 10^{-4} มิลลิเมตรต่อวินาทีและมีค่าประมาณ 0.3-0.5 เมกกะปาสคาลที่อัตราการเฉือนเท่ากับ 10^{-1} มิลลิเมตรต่อวินาที ส่วนค่ามุมเสียดทานจะมีค่าเพิ่มขึ้นประมาณ 2-5 องศา เมื่ออัตราการเฉือนเพิ่มขึ้นจาก 10^{-4} ถึง 10^{-1} มิลลิเมตรต่อวินาที ผลการวิจัยสามารถนำไปใช้ในการวิเคราะห์และออกแบบโครงสร้างทางวิศวกรรมในมวลหินที่รอยแตกอาจได้รับผลกระทบจากอัตราการเกิดแรงที่แตกต่างกันซึ่งเกิดขึ้นจากการเกิดแผ่นดินไหว การขุดเจาะและกิจกรรมจากการทำเหมือง

สาขาวิชา <u>เทคโนโลยีธรณี</u> ลายมือชื่อนักศึกษา______________________

ปีการศึกษา 2556 ลายมือชื่ออาจารย์ที่ปรึกษา________________

HASUN KODAE : EFFECT OF SHEAR RATE ON STRENGTH AND STIFFNESS OF SANDSTONE FRACTURES. THESIS ADVISOR : PROF. KITTITEP FUENKAJORN, Ph.D., P.E., 58 PP.

JOINT SHEAR STIFFNESS/JOINT SHEAR STRENGTH/SHEAR VELOCITIES/JOINT ROUGHNESS COEFFICIENT

The objective of this study is to determine the effects of shear velocity on the joint shear strengths and stiffness of fractures in sandstone. Specimens are prepared from the Phra Wihan, Phu Phan and Phu Kradung formations. The fractures are artificially made in the laboratory by tension inducing method. The fracture area is 90×100 mm^2. The normal stresses are maintained constant at 1, 2, 3 and 4 MPa. The shear velocities are varied from 10^{-4} to 10^{-1} mm/s. The results indicate that for all sandstone types the peak and residual shear strengths and joint shear stiffness increase exponentially with shear velocity, particularly under high normal stresses. Based on the Coulomb criterion cohesion can be as low as zero under the shear velocities of 10^{-4} mm/s to about 0.3-0.5 MPa under the shear velocities of 10^{-1} mm/s. The friction angles increase by about 2-5 degrees when the shear velocities increase from 10^{-4} to 10^{-1} mm/s. The findings are applicable to the analysis and design of engineering structures in rock mass where the joints are subjected to different loading rates induced, excavation and mining activities.

School of Geotechnology Student's Signature__________________

Academic Year 2013 Advisor's Signature_________________

ACKNOWLEDGEMENTS

The author wishes to acknowledge the support from the Suranaree University of Technology (SUT) who has provided funding for this research.

Grateful thanks and appreciation are given to Prof. Dr. Kittitep Fuenkajorn, thesis advisor, who lets the author work independently, but gave a critical review of this research. Many thank are also extended to Dr. Prachya Tepnarong and Dr. Decho Phueakphum, who served on the thesis committee and commented on the manuscript. Grateful thanks are given to all staffs of Geomechanics Research Unit, Institute of Engineering who supported my work

Finally, I would like to thank beloved parents and my wife for their love and most gratefully acknowledge friends for all their supported throughout the period of this research.

Hasun Kodae

TABLE OF CONTENTS

Page

TABLE OF CONTENTS (Continued)

Page

TABLE OF CONTENTS (Continued)

Page

LIST OF TABLES

LIST OF FIGURES

Figure **Page**

LIST OF FIGURES (Continued)

Figure **Page**

LIST OF FIGURES (Continued)

Figure **Page**

SYMBOLS AND ABBREVIATIONS

A	=	Empirical constant for equation (5.8)
c	=	Cohesion
d_n	=	Normal displacement
d_s	=	Shear displacement
I	=	Empirical constant for equation (5.3)
J	=	Empirical constant for equation (5.3)
JCS	=	Joint compressive strength
JRC	=	Joint roughness coefficient
κ	=	Empirical constant for equation (5.10)
K_s	=	Joint shear stiffness
L	=	Empirical constant for equation (5.9)
M	=	Empirical constant for equation (5.6)
N	=	Empirical constant for equation (5.6)
X	=	Empirical constant for equation (5.2)
Y	=	Empirical constant for equation (5.2)
α	=	Empirical constant for equation (5.9)
β	=	Empirical constant for equation (5.10)
$\delta d_s/\delta t$	=	Shear velocity
ϕ	=	Friction angle
ϕ_b	=	Basic friction angle

SYMBOLS AND ABBREVIATIONS (Continued)

σ_n	=	Normal stress
τ	=	Shear stress
$\dot{v}$	=	Rate of dilation at failure
ω	=	Empirical constant for equation (5.8)

CHAPTER I

INTRODUCTION

1.1 Background of problems and significance of the study

Joint shear strength is one of the important parameters that will be used in the analysis and design of engineering structures in rock mass. In jointed rock masses, joint surface properties such as roughness, separation and joint aperture have considerable effects on shear strength of rock joints. Several criteria have been proposed in the past to identify the strength of a rough rock joint under varied conditions. Knowledge and understanding of the shear velocity on the joint shear strength and dilation are however extremely rare.

1.2 Research objectives

The objective of this study is to determine the effects of shear velocity on the fracture shear strengths of sandstones. The fracture planes will be simulated in the laboratory using the tension-inducing method. The testing uses a true triaxial load frame. Rock samples are from the Phu Phan, Phu Kradung and Phra Wihan formations. Mathematical relationship between shear velocity and the joint shear strength and joint shear stiffness will be derived, which can be used to predict the mechanical stability of geo-engineering structures (e.g. foundation, slope and tunnel).

1.3 Research methodology

The research methodology shown in Figure 1.1 comprises 5 steps; including literature review, sample preparation and joint roughness scan, laboratory testing, data analysis, conclusions and thesis writing.

1.3.1 Literature Review

Literature review is carried out to study the previous researches on joint shear strengths under various shear velocities. The sources of information are from text books, journals, technical reports and conference papers. A summary of the literature review will be given in the thesis.

1.3.2 Sample Preparation

Sample preparation is carried out in the laboratory at the Suranaree University of Technology. Samples for the double shear planes test are prepared to have fractures area of about 90×100 mm^2. The fractures will be artificially made in the laboratory by tension inducing method. The joint roughness coefficient (JRC) for each fracture will be determined. A total of 12 samples is prepared for each shear velocity testing.

1.3.3 Laboratory Testing

The test method uses double shear plane technique as shown in Figure 1.2. The constant normal stresses on the fracture are 1, 2, 3 and 4 MPa. The test is terminated when a total of 5 mm of shear displacement is reached. The shear velocities vary from 1×10^{-1} to 1×10^{-4} mm/s.

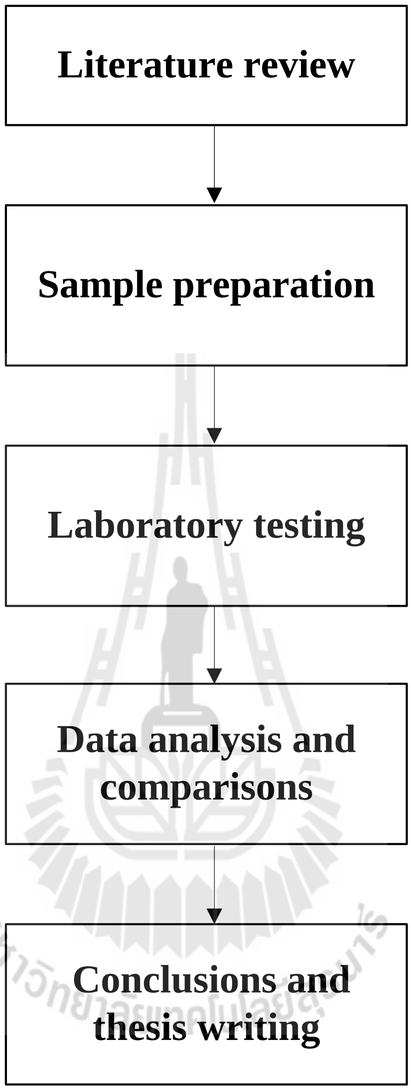

Figure 1.1 Research Methodology

1.3.4 Determination of Dilation, Friction Angle and Cohesion

Test results will be used to determine the joint shear stiffness from shear stress and displacement curves. By applying the Coulomb criterion friction angle and cohesion will be determined from the normal and shear stress relations at the peak and residual regions.

1.3.5 Development of Mathematical Relations

Results from laboratory test are used to formulate mathematical relations between the joint shear strengths, shear velocities, joint shear stiffness and normal stress. Such equation will be useful for determining the shearing resistance of functions under different shear velocities.

1.3.6 Discussions

The research results are discussed and comparison with another research.

1.3.7 Conclusions and Recommendation for Future Studies

The research method and discuss are conclusion and provides recommendations for future studies.

1.3.8 Thesis Writing

All research activities, methods, and results are documented and complied in the thesis. The research or findings will be published in the journals**.**

1.4 Scope and Limitations of the Study

The scope and limitations of the research include as follows.

1. Laboratory testing is conducted on sandstone specimens from the Phra Wihan, Phu Kradung and Phu Phan fomations.

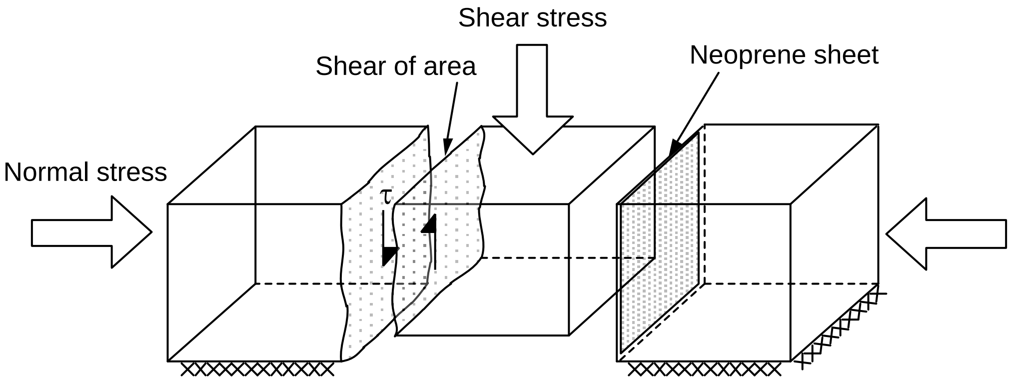

Figure 1.2 Double shear plane technique.

2. The applied normal stresses (σ_n) vary from 1, 2, 3 to 4 MPa.
3. The applied shearing velocity ($\delta d_s/\delta t$) vary from 10^{-1} to 10^{-4} mm/s.
4. Up to 16 samples are tested, with the nominal sample size of 100×100×225 mm^3.
5. Testing is made under dry condition.
6. All tests are conducted under ambient temperature.
7. No fields testing are conducted.

1.5 Thesis contents

Chapter I introduces the thesis by briefly describing the background of problems and significance of the study. The research objectives, methodology, scope and limitations are identified. **Chapter II** summarizes results of the literature review. **Chapter III** describes the sample preparation and laboratory experiment. **Chapter IV** presents the results obtained from the laboratory testing. **Chapter V** developed mathematic relations. **Chapter VI** is discussion of the results. **Chapter VII** are concludes the research results, and provides recommendations for future research studies.

CHAPTER II

LITERATURE REVIEW

2.1 Introduction

This chapter summarizes the results of literature review carried out to improve an understanding of effect of shear rate, shear velocity, joint shear strength criteria, effect of loading rate on intact rock and effect of joint roughness.

2.2 Effect of Shear Rate and Shear Velocity

Frictional resistance of rock joints is dependent of the rate of shear displacement. The magnitude of this effect is quite variable, depending mainly on the rock type and normal stress level. In general, for harder rocks, the frictional resistance has been found to decrease with increasing shear displacement rates greater than a variable critical velocity (Crawford and Curran, 1981).

Vasarhelyi (1998) has studied the influence of normal load on joint dilatation rate. The results show that the measured dilatation angle decreases with the increased normal force and it is always present. However, the Equation 2.1 is also correct for the cases when the Patton and the Seidel and Haberfield equations fail.

$$\tau = \sigma_n \tan (\phi_\mu + \dot{v}) \qquad (2.1)$$

where ϕ_μ = basic friction angle and $\dot{v}$ = the rate of dilation at failure. This means that this is a more general equation and it should be valid until the ‘‘teeth’’ (or irregularities) are not shorn off. This point is not at the transition stress, rather the meeting point of the

Jaeger curve and the bilinear curve. The measured dilatation-displacement curves show that, after the peak stress, the rate of dilatation does not change until a lot later.

Jafari et al. (2003) have studied the effects of displacement rates (or shearing velocity) on shear strength, some monotonic tests were performed in different ranges of axial displacement in 4 MPa confining pressure from 0.05 to 0.4 mm/s. The differences between the curves can be related to the effects of shear velocity on second-order asperities, as the total applied displacement is limited. It is observed that shear strength reduces with increasing shear velocity, approaching the same values for the peak and residual strength at higher shearing velocities.

Park and Song (2009) perform direct shear test on a rock joint using a bonded-particle model. The normal stresses applied to the sample were 3 and 15 MPa, which are approximately 2% and 10% of the uniaxial strength of the intact sample, respectively. The shear stress increased rapidly until the peak strength was passed, and reached some residual value that remained constant as the displacement continued. The peak and residual strengths were 5.33 and 1.82 MPa at low normal stress and 15.5 and 5.77 MPa at high normal stress. The friction calculated from the ratio of the peak shear strength to the given normal stress was higher at lower normal stress: 1.78 at 3 MPa and 1.03 at 15 MPa. The rate of change in normal displacement showed a maximum value at the peak shear stress level and decreased gradually in both cases. The normal displacement continued to increase at low normal stress, while it convergedat high normal stress when the residual state reached. The normal displacements at a shear displacement of 1.6 mm were 0.795 mm at 3 MPa and 0.434 mm at 15 MPa. These are approximately 2.21% and 1.21% of the sample height of 36 mm, respectively. There were a larger number of normal cracks(tensile cracks) than the shear cracks, and the total number increased with increasing normal stress: 650 cracks at 3 MPa and 3290 at 15 MPa. For reference, the number of joint contacts was 5,196 at the initial stage. The cracks were initiated at 80% of the peak (pre-peak), and propagated rapidly until the shear stress reached 80% of the peak stress after passing the peak (post-peak). After the first crack was initiated, the shear stress showed a non-linear relationship with the shear displacement.

2.3 Joint Shear Strength Criteria

Coulomb criterion represents the relationship between the peak shear strength and normal stress by costs include costs of sample maintain, transport, prepares, and testing.

$$\tau = c + \sigma_n \tan\phi \tag{2.2}$$

where τ is joint shear strength, σ_n is normal stress, c is the cohesive strength, and ϕ is angle of friction. These factors are the laboratory result. The result may not agree with rock mechanics work under high compressive strength. This is because of the relationship between τ and σ_n of Coulomb criterion is linear while actual relation is curve.

Barton (1973) has studied the behavior of natural rock joints and proposed a criterion that is modified from Patton. It can be re-written as

$$\tau = \sigma_n \tan \{\phi_B + \mathrm{JRC} \log_{10} (\sigma_j / \sigma_n)\} \tag{2.3}$$

where τ is joint shear strength, ϕ_B is basic friction angle, σ_n is normal stress, JRC is the joint roughness coefficient, and JCS is the joint wall compressive strength. Joint

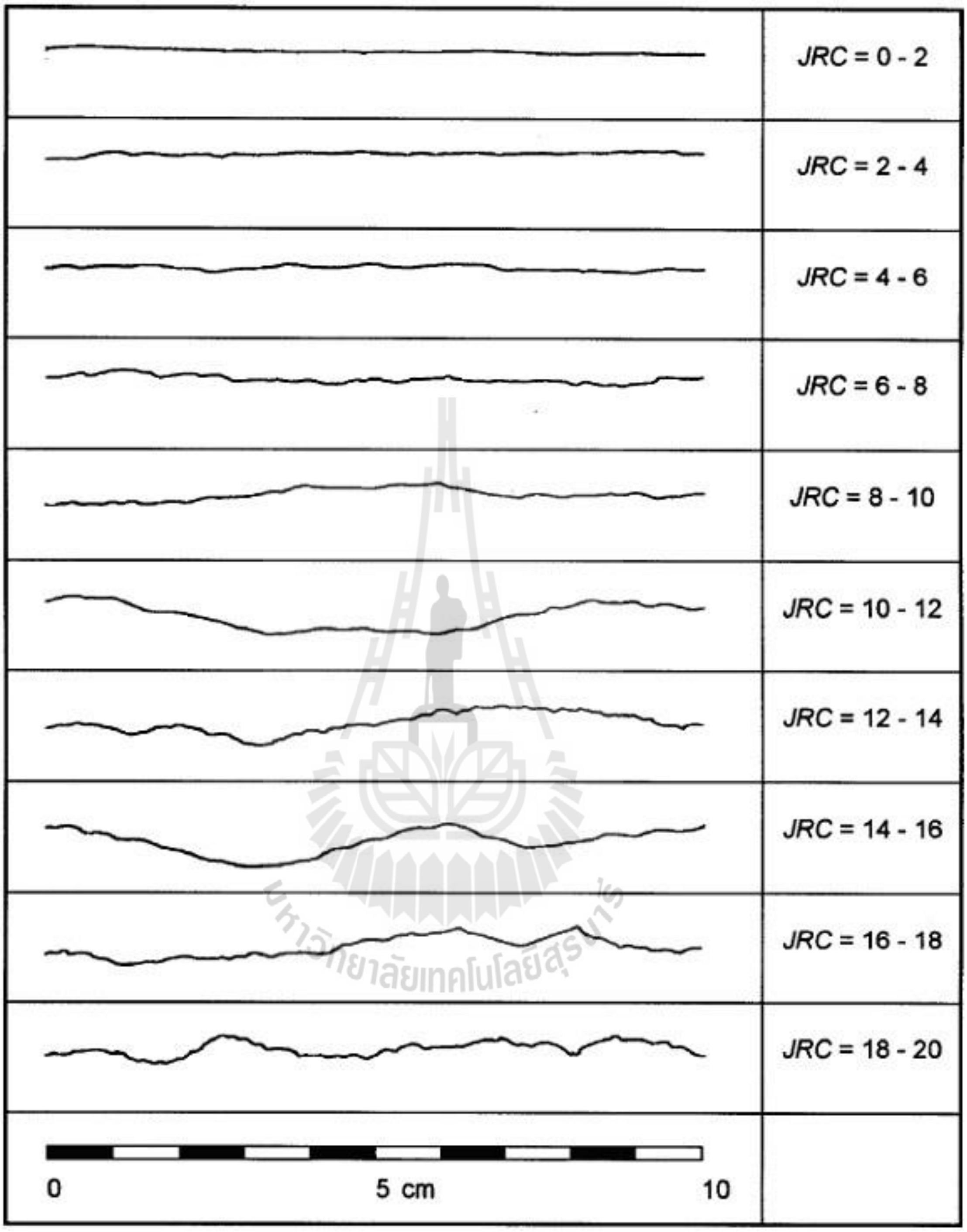

Figure 2.1 Roughness profiles and corresponding JRC values (Barton 1973).

roughness coefficient can correlate with Figure 2.1.

2.4 Effect of Loading Rate on Intact rock

Sangha and Dhir (1972) studied the influence of strain rate on the strength, deformation and fracture properties of Lower Devonian sandstone. Strain rates were varied between 2.5×10^{-3}/sec to 2.5×10^{-9}/sec. They suggested a new criterion, based on the incremental Poisson's ratio, capable of predicting both the long-term strength of a material and also able to establish whether a material under load is safe from long-term failure. This criterion was based on short-term creep tests and substantiated by the constant strain-rate strength results. Comparison of strength results obtained at different rates of loading and rates of straining showed that for similar loading times to failure the constant rates of loading gave slightly higher strength values. Modes of rupture were found to be independent of both loading methods but dependent upon time taken to reach strength failure.

Ma and Daemen (2006) study the strain rate dependent strength and stress-strain characteristics of a welded tuff. Results of 61 uniaxial compression tests on the welded Topopah Spring tuff are presented. The tests were carried out under constant strain rates at room temperature. Stress–strain analysis indicates that dilatancy and compaction start at about 50% of ultimate strength. A sudden stress drop occurs at about 90% of the ultimate strength, which indicates the onset of specimen failure. Both strength and peak axial strain decrease with strain rate as power functions. Based on the strain rate dependence of strength and peak axial strain, it is inferred that the elastic modulus is strain rate dependent. A relationship between stress, axial strain, and axial strain rate is developed. The parameters in this relation are estimated using multivariate regression to fit stress–axial strain–strain rate data.

Kenkhunthod and Fuenkajorn (2010) study the influence of loading rate on deformability and compressive strength of three Thai sandstones. Uniaxial and triaxial compressive strength tests have been performed using a polyaxial load frame to assess the influence of loading rate on the strength and deformability of three Thai sandstones. The applied axial stresses are controlled at constant rates of 0.001, 0.01, 0.1, 1.0 and 10 MPa/s. The confining pressures are maintained constant at 0, 3, 7 and 12 MPa, as shown in Figure 2.2. The sandstone strengths and elastic moduli tend to increase exponentially with the loading rates. The effects seem to be independent of the confining pressures. An empirical loading rate dependent formulation of both deformability and shear strength is developed for the elastic and isotropic rocks. It is based on the assumption of constant distortional strain energy of the rock at failure under a given mean normal stress. The proposed multiaxial criterion well describes the sandstone strengths within the range of the loading rates used here. It seems reasonable that the derived loading rate dependent equations for deformability and shear strength are transferable to similar brittle isotropic intact rocks.

Ray et al. (1999) describe the effect of cyclic loading and strain rate on the mechanical behaviour of sandstone. The results indicate that the percentage decrease in uniaxial compressive strength was found to increase with the increase in applied stress level and direct proportionality between the two parameters was found. The uniaxial compressive strength of Chunar sandstone was determined at strain rates of 2.5×10^{1}/s, 2.5×10^{0} and 2.5×10^{-1}/s and found to be 99.5 MPa, 75.1 MPa and 64.0 MPa, respectively (Figure 2.3). A clear increase in uniaxial compressive strength was, therefore, observed with increase in strain rate. The failure strength was found to increase with the increase of strain rate and an abrupt increase in strength was noticed at the strain rate of 2.5×10^{1}/s. Fatigue stress was found to increase with the increase in strain rate and Young's modulus was found to increase with the increase in strain rate (Figure 2.4).

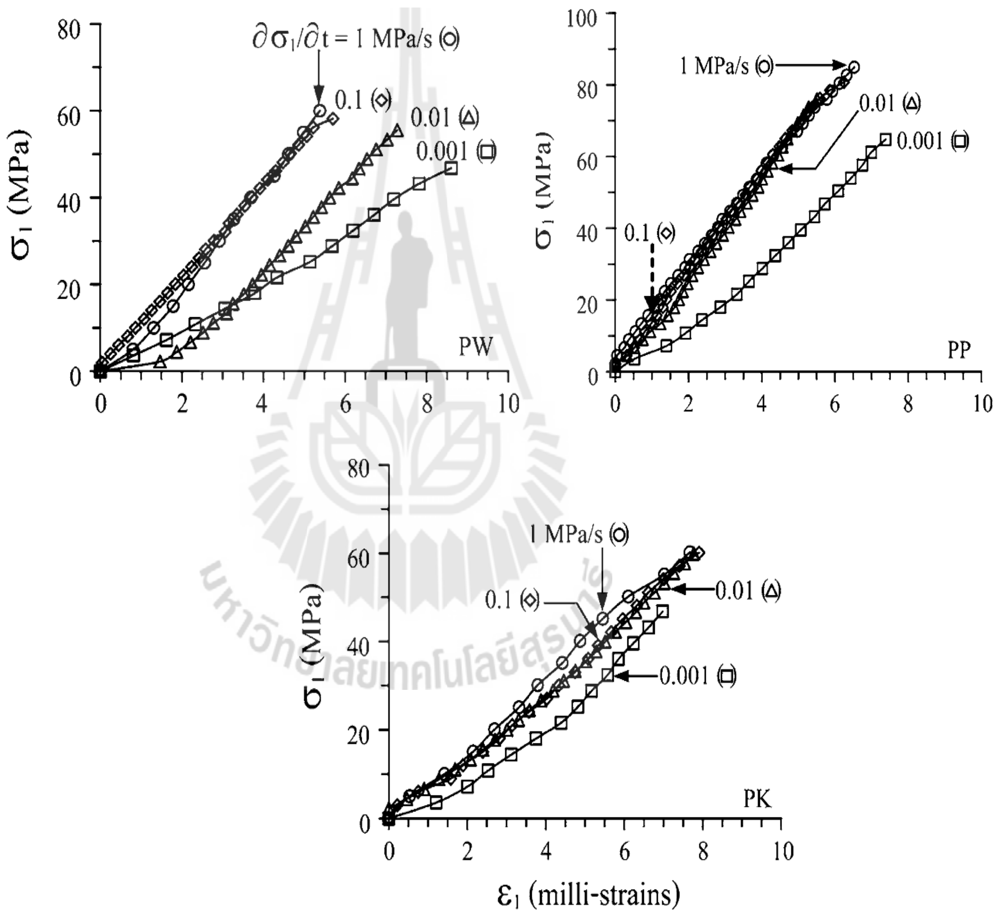

Figure 2.2 Uniaxial compressive strengths under loading rates varied from 0.001, 0.01, 0.1 and 1.0 MPa/s, for PW, PP and PK sandstones (Kenkhunthod and Fuenkajorn, 2010).

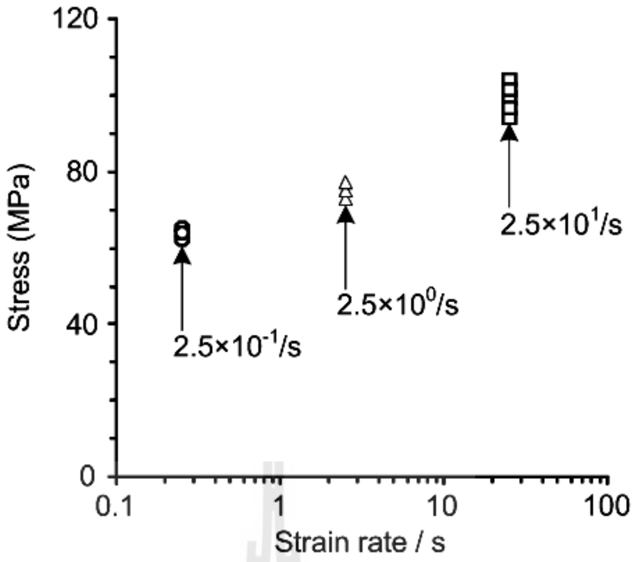

Figure 2.3 Stress as function of strain rate (Ray et al., 1998).

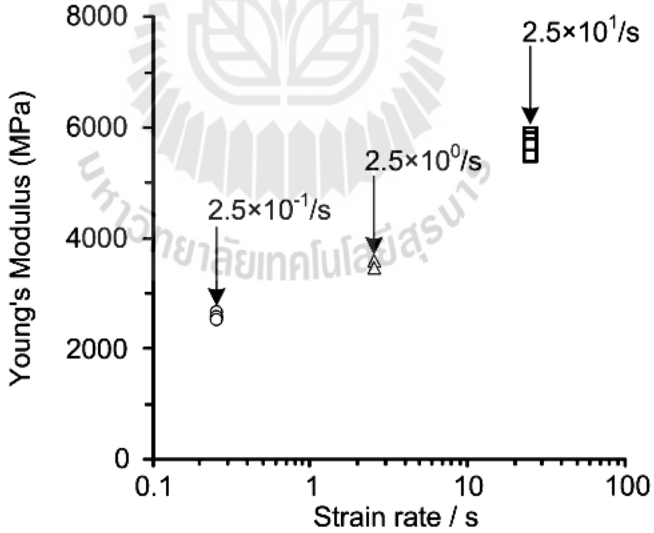

Figure 2.4 Young's modulus as function of strain rate (Ray et al., 1998).

2.5 Effect of Joint Roughness

Kwafniewski and Wang (1997) have studied the surface roughness evolution and mechanical behavior of rock joints under shear. The shear behavior of rock joints characterized by the shear stiffness and peak shear strength depends mainly on the normal load applied. The shear stiffness and shear strength have relatively smaller values. Experiments show a complex dependence of shear stiffness and the peak shear strength on the roughness. The shear behavior of rock joints characterized by the shear stiffness and peak shear strength depends mainly on the normal load applied. Experimental results show that, at a lower θ, the shear stiffness and shear strength have relatively smaller values. In such a case, the shear resistance drops once the peak shear strength has been achieved. At a higher θ, however, both shear stiffness and the peak shear strength significantly increase and the drop in shear resistance after the peak shear strength becomes more evident. For $\theta = 45°$, i. e. high normal force conditions, a number of significant peaks have been normally recorded in the post-initial yield region. When subjected to normal and tangential loads, the rough surfaces of rock joints experience damage in the process of shearing. The failure mode of asperities on the joint surfaces and the degradation of surface structure depend on the normal force applied as well as the shear history. The physical process of surface damage is in fact considerably complex. Due to the random character of surface structure, it is quite possible that the damage of a rough surface occurs as a result of several mechanisms. For instance, tensile split occurs at steeper asperities in one part, while sliding or rotation of failed asperities in another part of the joint. Moreover, in some sequences, individual mechanisms of surface damage may take place in the loading history. The observed macrochanges in the surface topography actually tell only a part of the story of the damage process.

Lee et al. (2001) proposed a cyclic shear testing system that was established to investigate the mechanical behavior of rough rock joints under cyclic loading conditions. Laboratory cyclic shear tests were conducted for two joint types of Hwangdeung granite and Yeosan marble, saw-cut and split tensile joints. Prior to the test, the roughness of each specimen was characterized by measuring the surface topography using a laser profilometer. Monotonic shear behaviors of rough joints were simulated using the proposed model in this study. Input parameters were obtained based on the results of laboratory tests. Initial asperity angles and damage coefficients were also calculated from the results of laser profilometer analysis and asperity degradations. Simulated shear behaviors of three rough joint specimens are superimposed on the laboratory test results. The proposed model precisely simulated the peak shear stresses and the shear stress–shear displacement relations from numerical simulations were closely matched with the laboratory test results. Simulated dilation curves could also replicate the general trend of nonlinear changes for rough joint as discovered in the experimental results.

Seidel and Haberfield (2002) investigated the behaviour of rock joints subjected to direct shear. Both concrete/rock and rock/rock joints were investigated. The behaviour of rock/rock joints is important for the assessment of stability issues involving rock masses (e.g. rock slope stability). Concrete/rock joints are vital to the assessment of performance of concrete piles socketed into rock, rock anchors and concrete dam foundations. Initially, before the commencement of sliding, the two halves of the joint are assumed to be in intimate contact with both faces of each asperity in full contact. After the initiation of interface slip, the contact area between the two halves of the joint is restricted to one asperity face, and progressively reduces as shear displacement progresses. This is demonstrated in Figure 2.5 for an interface comprising regular triangular asperities. Local normal stresses increase both as a consequence of the reduced contact area and as a result of the increasing normal stress due to the constant normal stiffness (CNS) condition. A critical normal stress is reached at which the asperity can no longer sustain the loading and individual asperity failure results. The asperity shearing mechanism was observed to differ between Johnstone/Johnstone (J/J) and Johnstone/Concrete (J/C) joints. For J/C joints, the much stronger half of the joint constrained failure over the full contact length of each asperity. However, for J/J joints the material on both sides of the interface is similar, allowing failure to occur at localized regions of high stress that occur at the leading and trailing points of contact of each asperity. Failure gradually progressed from these localized regions until complete failure of each asperity (and therefore of the whole interface) occurred. This resulted in a significant reduction in the measured strength. The finite difference program FLAC was used to investigate the failure of both J/J and J/C interfaces. The results of this analysis indicated that the ultimate failure mode in J/J joints was similar to that of J/C joints, but failure occurred at a lower stress. A stress reduction factor of 1.38 was found to be appropriate for J/J joints.

Kemeny (2003) developed a fracture mechanics model to illustrate the importance of time dependence for brittle fractured rock. In particular a model is developed for the time dependent degradation of rock joint cohesion. Degradation of joint cohesion is modeled as the time-dependent breaking of intact patches or rock bridges

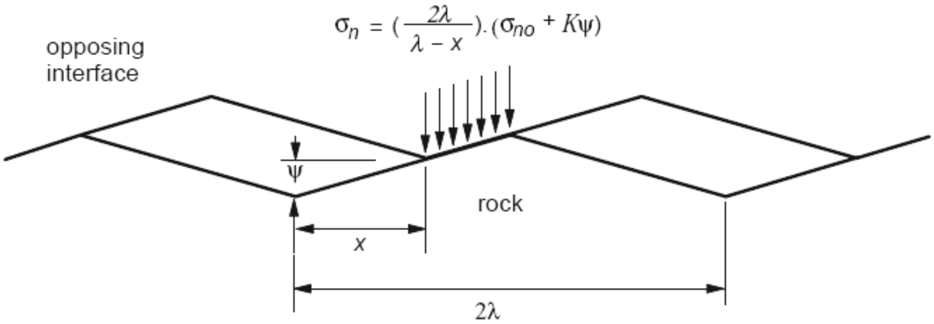

Figure 2.5 Reduction of asperity contact area with progressive shear displacement (Seidel and Haberfield, 2002).

along the joint surface. A fracture mechanics model is developed utilizing subcritical crack growth, which results in a closed-form solution for joint cohesion as a function of time. As an example, a rock block containing rock bridges subjected to plane sliding is analyzed. The cohesion is found to continually decrease, at first slowly and then more rapidly. At a particular value of time the cohesion reduces to value that result in slope instability. A second example is given where variations in some of the material parameters are assumed. A probabilistic slope analysis is conducted, and the probability of failure as a function of time is predicted. The probability of failure is found to increase with time, from an initial value of 5% to a value at 100 years of over 40%. These examples show the importance of being able to predict the time dependent behavior of a rock mass containing discontinuities, even for relatively short-term rock structures.

Kemthong and Fuenkajorn (2007) perform direct shear test on saw-cut specimens to determine the relationship between the basic friction angle (ϕ_b) and the rock compressive strength (UCS). Testing on specimens with tension-induced fractures yielded joint shear strengths under different JRC's for use in the verification. The results indicate that Barton's criterion using the field-identified parameters can satisfactorily predict the shear strengths of rough joints in marble and sandstones, and slightly over-predicts the shear strength in the basalt specimens. It cannot however describe the joint shear strengths for the granite specimens. This is probably because the saw-cut surfaces for coarse-grained and strong crystalline rocks are very smooth resulting in an unrealistically low ϕ_b. Barton's shear strength criterion is more sensitive to ϕ_b than to UCS and JRC. For all sandstones the ϕ_b values are averaged as 33 ± 8 degrees, apparently depending on their cementing materials. The average ϕ_b for the tested marbles and for the limestone recorded elsewhere 35 ± 3 degrees, and is independent of UCS. The ϕ_b values for other rock types apparently increase with UCS particularly for very strong rocks. The factors governing ϕ_b for crystalline rocks are probably crystal size, mineral compositions, and the cutting process, and for clastic rocks are grain size and shape and the strength of cementing materials.

CHAPTER III

SAMPLE PREPARATION

3.1 Introduction

This chapter describes the rock sample preparation. The rock samples include Pra Wihan, Phu Kradung and Phu Phan sandstones (here after designated as PW, PK and PP sandstones) (Figure 3.1). These rocks have significant impacts on stability of many engineering structures constructed in region (slope embankments, underground mines and tunnels). They are selected here due to their uniform texture and availability.

3.2 Sample preparation

Sixteen specimens are prepared for each rock type. The sample preparation is carried out in the laboratory at the Suranaree University of Technology. Specimens for shear test are prepared to have fractures area of about 100×90 square millimeters. The fractures are artificially made in the laboratory by tension inducing in 100×100×225 mm^3. Samples comprise 3 blocks. Each block has a dimension of 100×100×75 mm^3 (Figure 3.2). These rocks are classified as fine-grained quartz sandstones with highly uniform texture and density. Their roughness is observed and classified by comparing with a reference profiles given by Barton (joint roughness coefficient-JRC, Barton, 1973). For all sandstone specimens the joint roughness coefficients of the tension-induced fractures are in the range between 6 and 12. Figure 3.3 shows the joint roughness of rock samples.

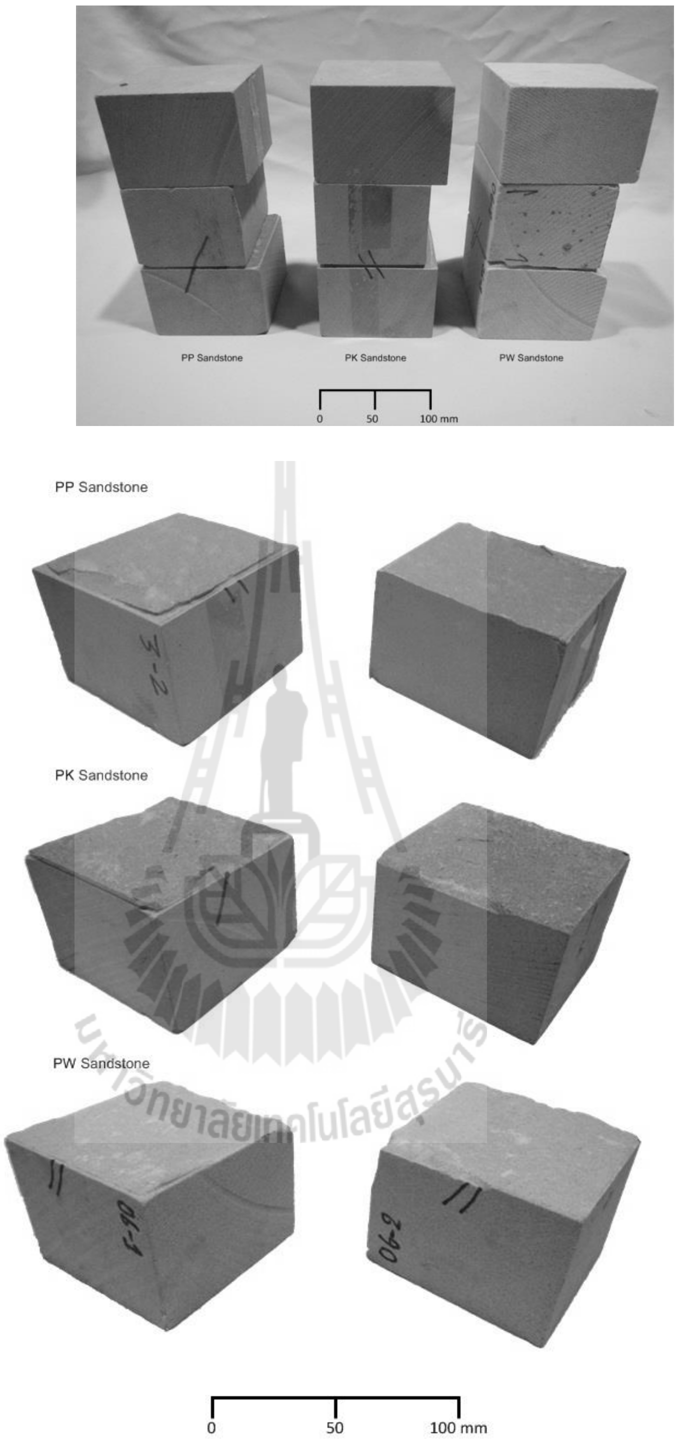

Figure 3.1 Some rock specimens prepared for double shear plane.

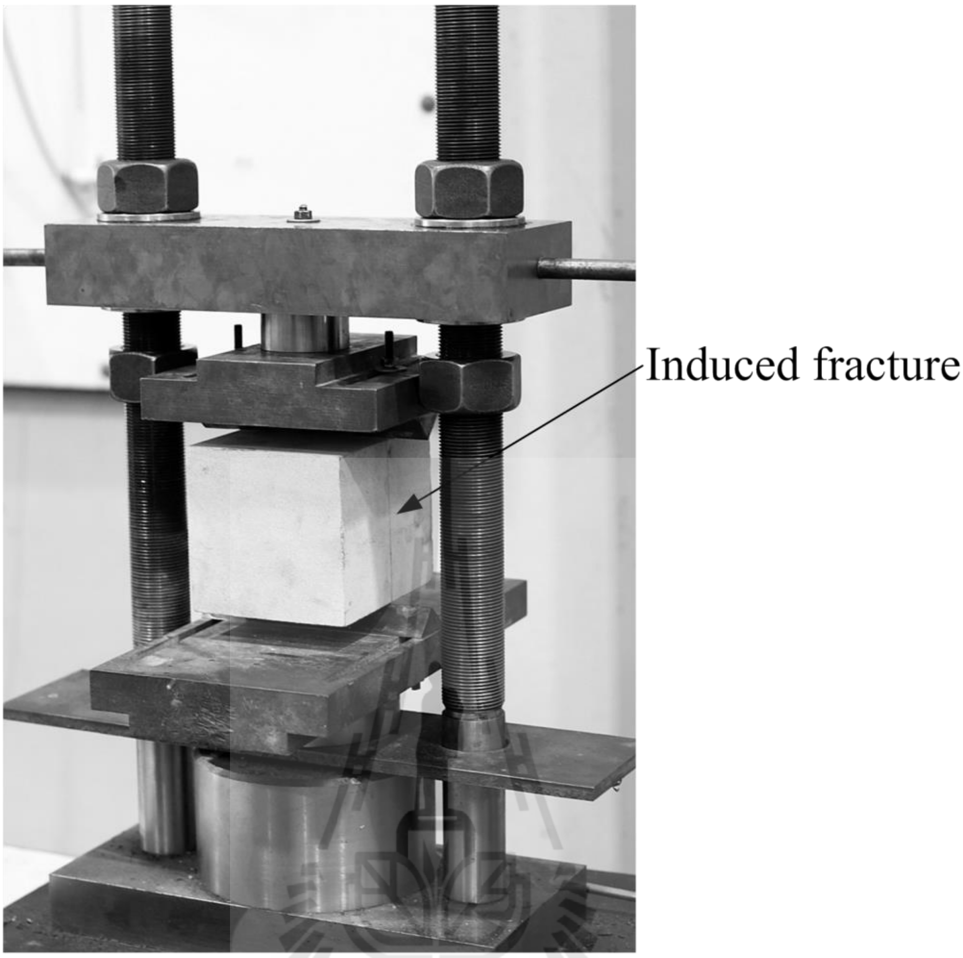

Figure 3.2 100×100×225 cubic millimeters block of rock sample is line-loaded to induce tensile fracture.

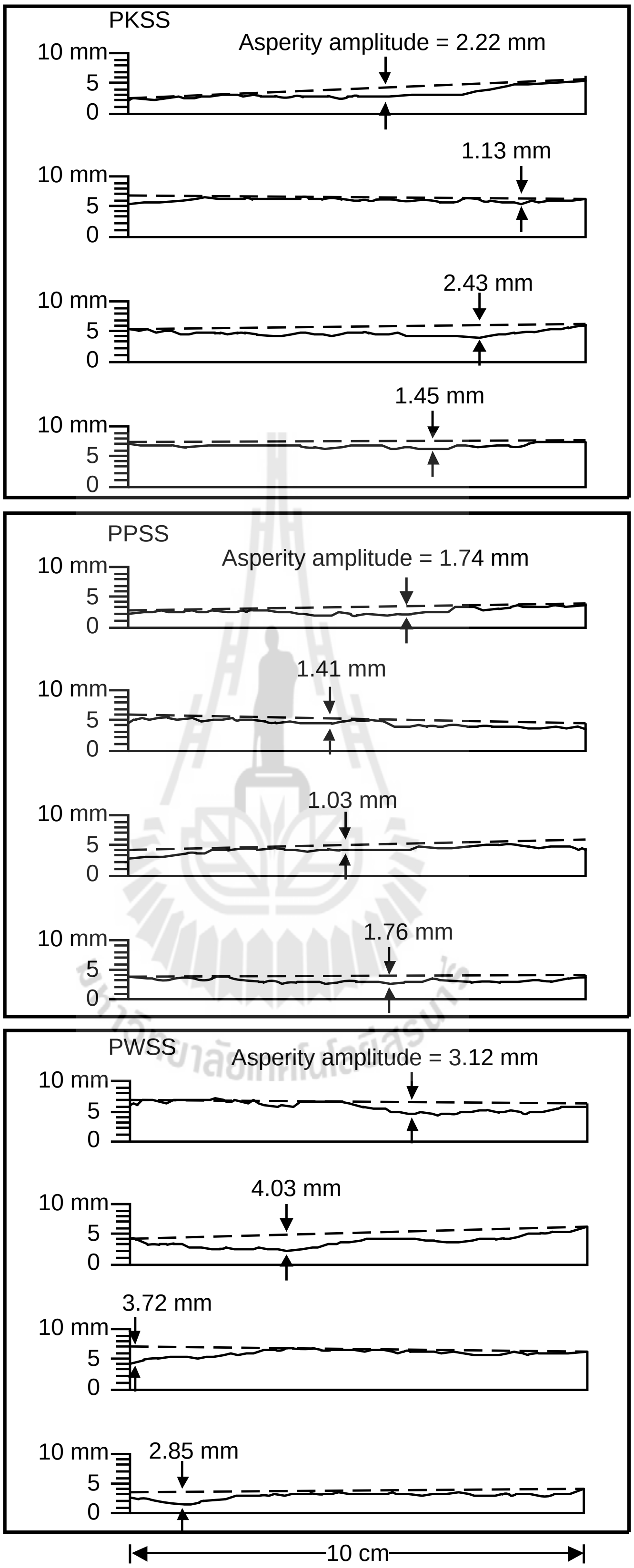

Figure 3.3 Joint roughness coefficient (JRC) of PK, PP and PW. (JRC = 7, 6 and 12)

Table 3.1 Joint roughness coefficient (JRC) of some specimens PK, PP and PW sandstones.

Rock type	Sample no.	Joint roughness coefficient (JRC)	Average
PK	01-01	7	7
	02-01	6	
	04-01	7	
	06-01	7	
	08-01	8	
	12-01	7	
	15-01	7	
	18-01	7	
PP	01-01	6	6
	03-01	6	
	04-01	6	
	05-01	6	
PW	01-01	11	12
	04-01	13	
	05-01	13	
	06-07	12	
	08-01	12	
	10-01	11	
	11-01	12	
	16-01	12	
	18-01	12	

CHAPTER IV

LABORATORY TESTING

4.1 Introduction

The objective of the laboratory testing is to assess the effects of shear velocity on fracture shear strengths by performing series of double fracture shear testing on tension-induced fractures in Phu Phan, Phu Kradung and Phra Wihan sandstone specimens.

4.2 Test Method

4.2.1 Equipment

A true triaxial load frame is used to apply true triaxial stress to the specimens (Figure 4.1). The true triaxial load frame has has mutually perpendicular 3 pair of steel plates. Four pillars secure each pair. Each pair has spacing about 61 cm^2. The steel plates have dimension of $43\times43\times4$ cm^3 and other two are $30\times30\times6$ cm^2. Six hydraulic load cells have capacity of 10,000 psi. Diameter of hydraulic load cell is 9 cm^2. One of the lateral stresses (horizontal) is set perpendicular to the fractures plane, which is designated as normal stress (σ_n). The shear stress (τ) is applied by top hydraulic load cell. The bottom hydraulic pump is fixed. Two dial gages are used for monitoring the normal and shear displacement, as shown in Figure 4.2.

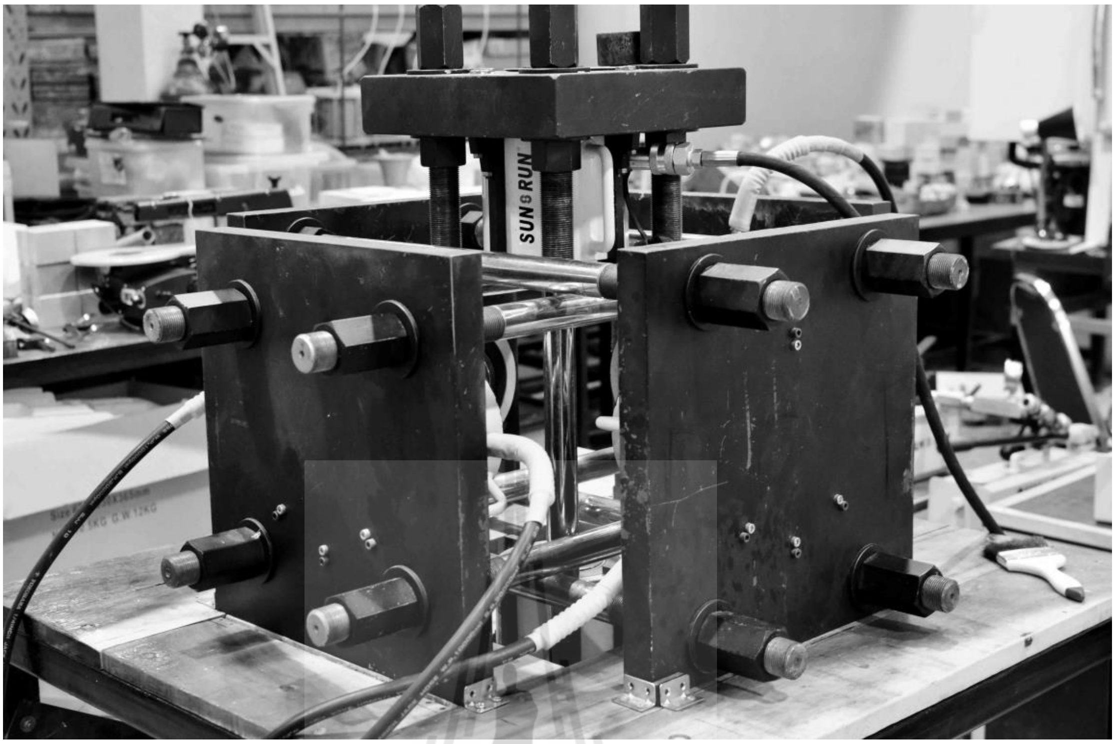

Figure 4.1 True triaxial load frame.

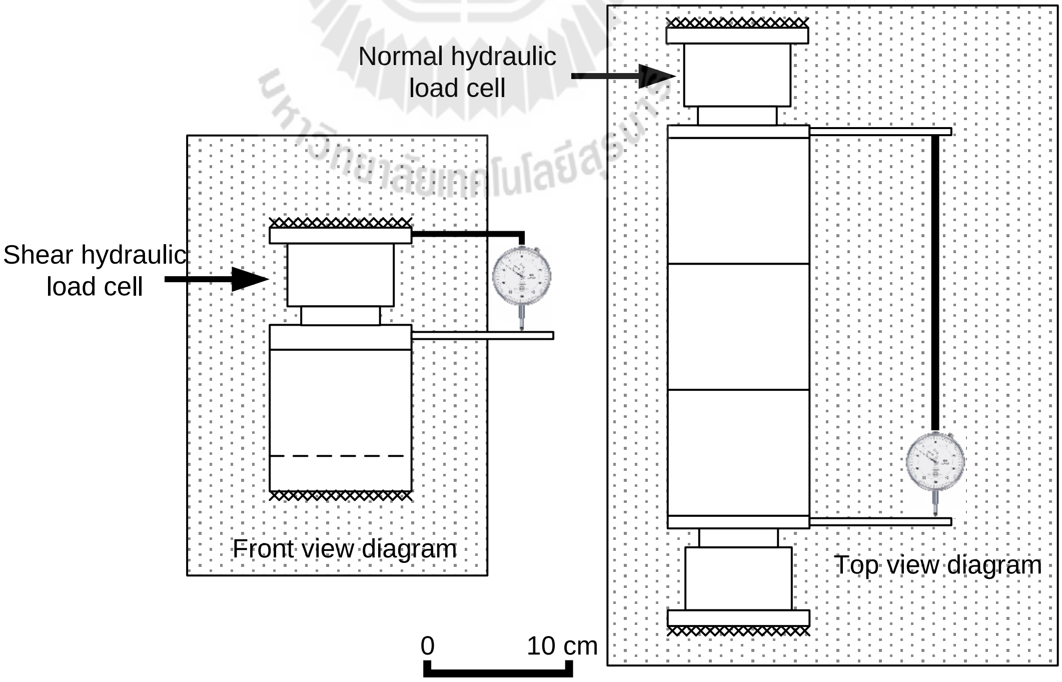

Figure 4.2 Test configurations.

4.2.2 Testing procedure

The tests are performed with the normal stresses of 1, 2, 3 and 4 MPa for the rough fractures. Each specimen is sheared only once under the predefined constant normal stress. Figure 4.3 shows the laboratory arrangement of the double shear plane test while the fracture is under normal and shear stresses. The shearing velocities are 0.0001, 0.001, 0.01 and 0.1 mm/s. The shear force is continuously applied until a total shear displacement of 5 mm is reached. The applied normal and shear forces and the corresponding normal form and shear displacements are monitored and recorded. Figure 4.4 shows the pre-test and post-test fractures for the PK PP and PW sandstones.

4.3 Test Results

Figures 4.5 through 4.7 show shear stresses of PK, PP and PW sandstones as a function of shear displacement for various shear velocities ($\delta d_s/\delta t$). Figures 4.8 through 4.10 show shear displacements of PK, PP and PW sandstones as a function of normal displacements for various shear velocities ($\delta d_s/\delta t$). Tables 4.1 lists the peak and residual shear stresses for all specimens. The higher the shear velocity applied, the higher the peak and residual shear stresses are obtained. Figure 4.11 show the peak and residual shear stresses of PW, PK and PP sandstones as a function of normal stress for various shear velocities ($\delta d_s/\delta t$). Table 4.2 shows joint shear stiffness for all specimens. Figure 4.12 show the joint shear stiffness as a function of normal stress for various shear velocity ($\delta d_s/\delta t$) and as a function of rate for various normal stress (σ_n). The higher shear velocities and normal stress result in higher joint shear stiffness obtain. The higher joint roughness coefficients (JRC) lead to the high shear strength.

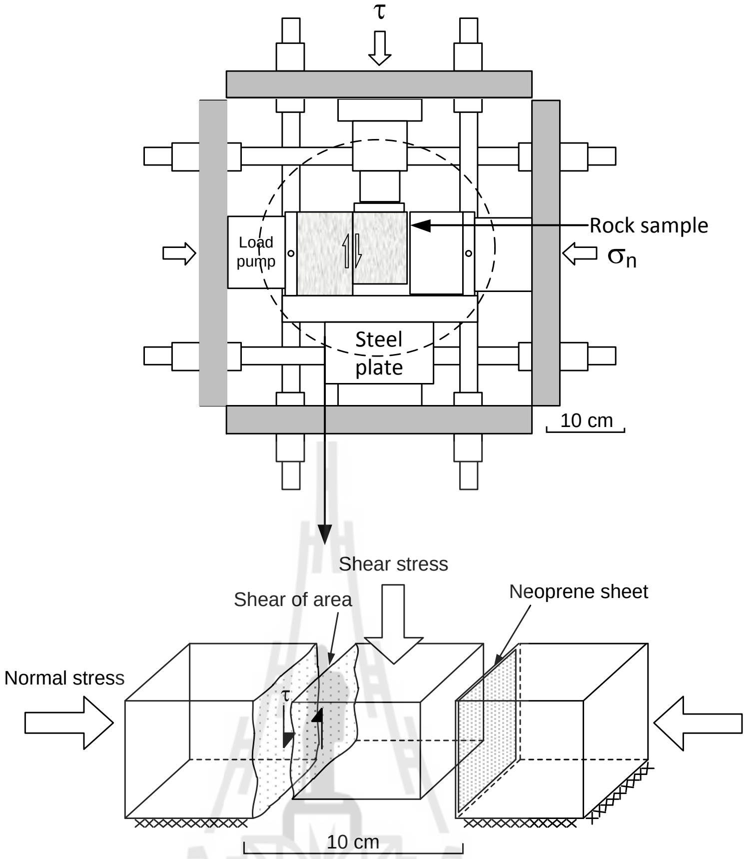

Figure 4.3 Diagram while double shears testing.

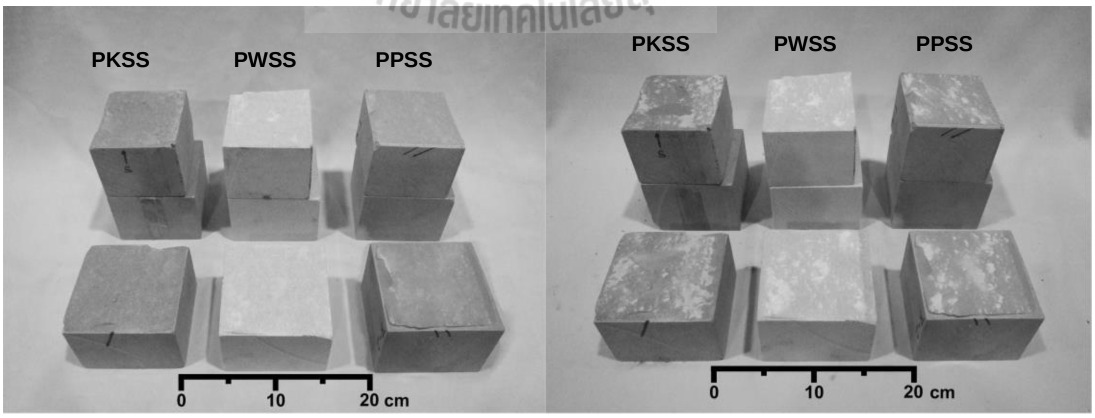

Figure 4.4 Pre and post-test PK, PW and PP sandstones.

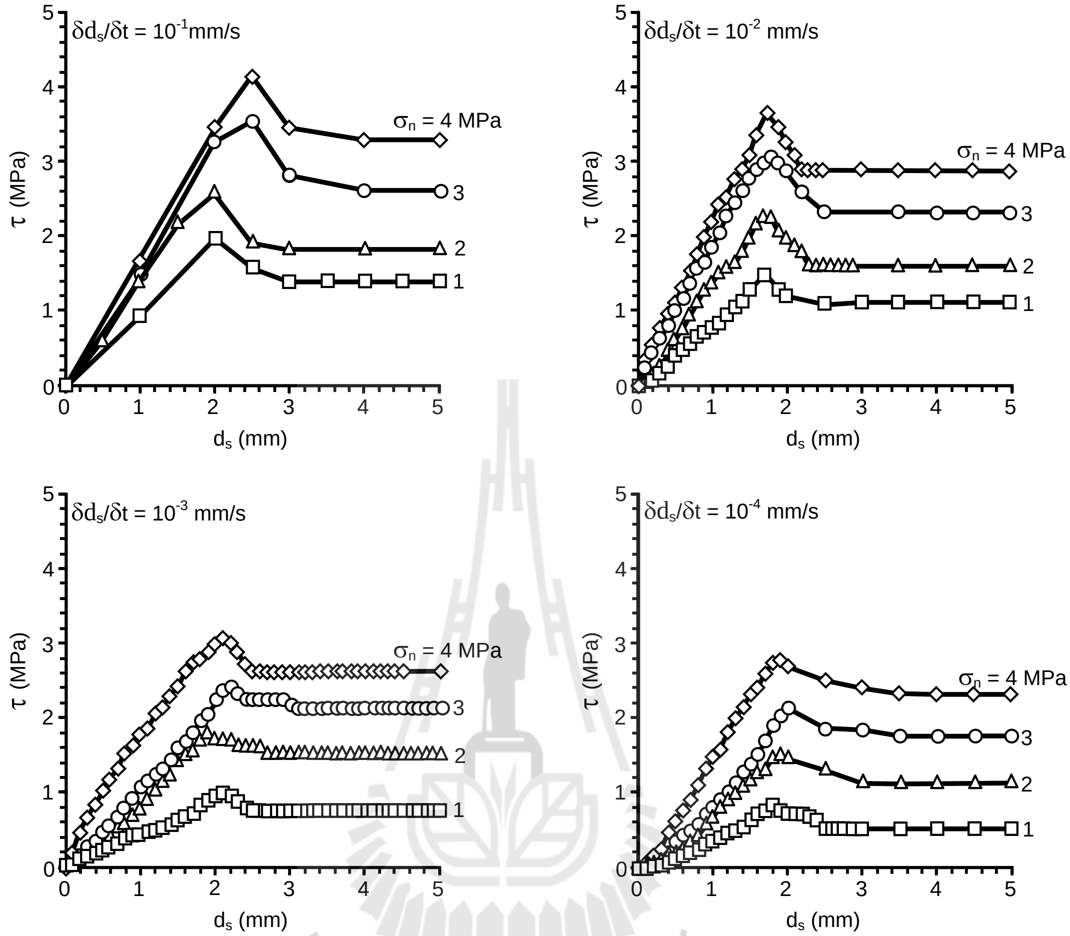

Figure 4.5 Shear stresses (τ) of PK sandstone as a function of shear displacement (d_s).

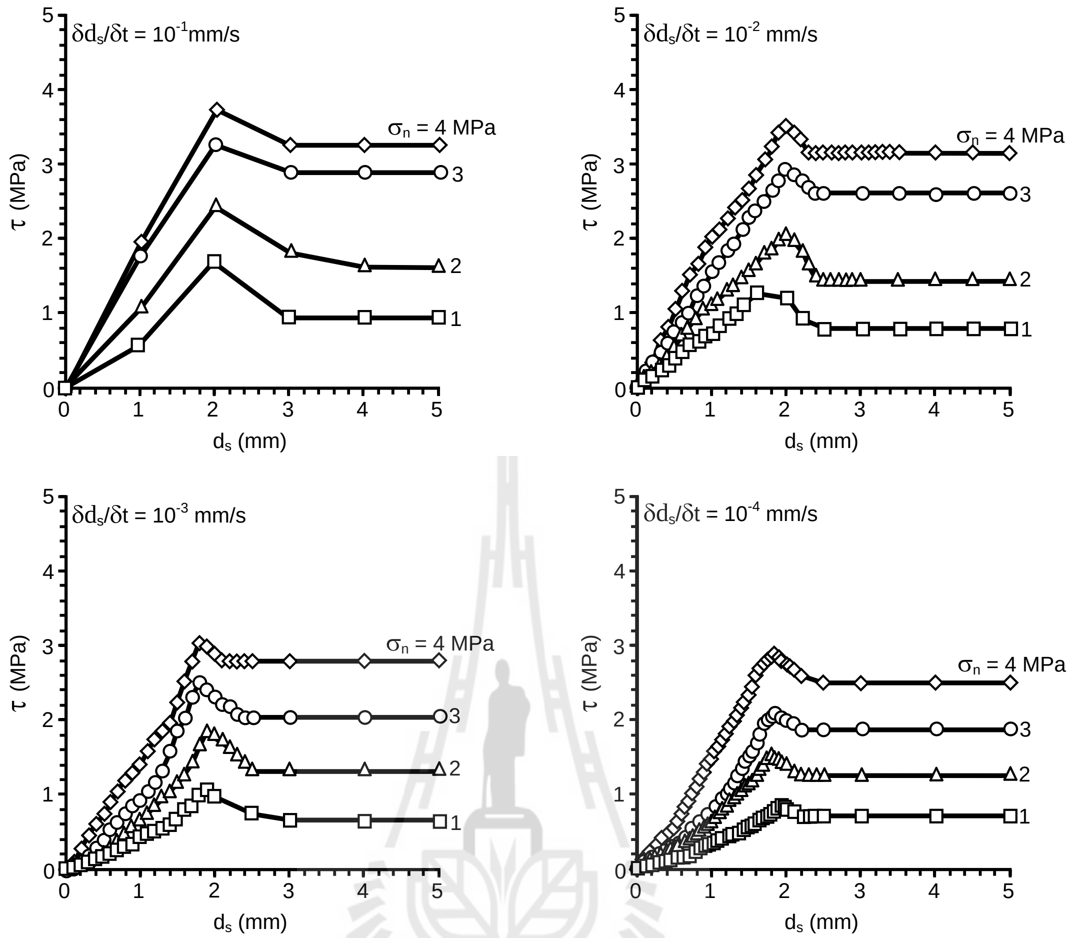

Figure 4.6 Shear stresses (τ) of PP sandstone as a function of shear displacement (d_s).

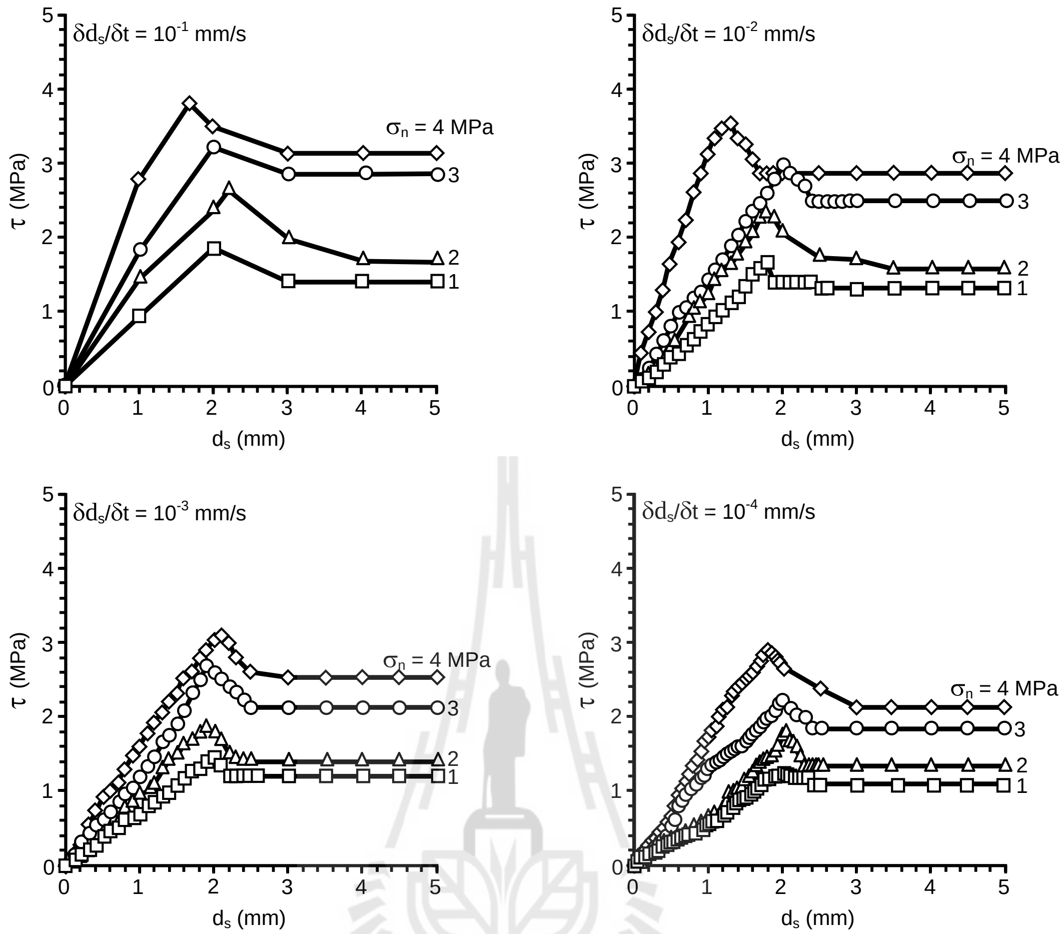

Figure 4.7 Shear stresses (τ) of PW sandstone as a function of shear displacement (d_s).

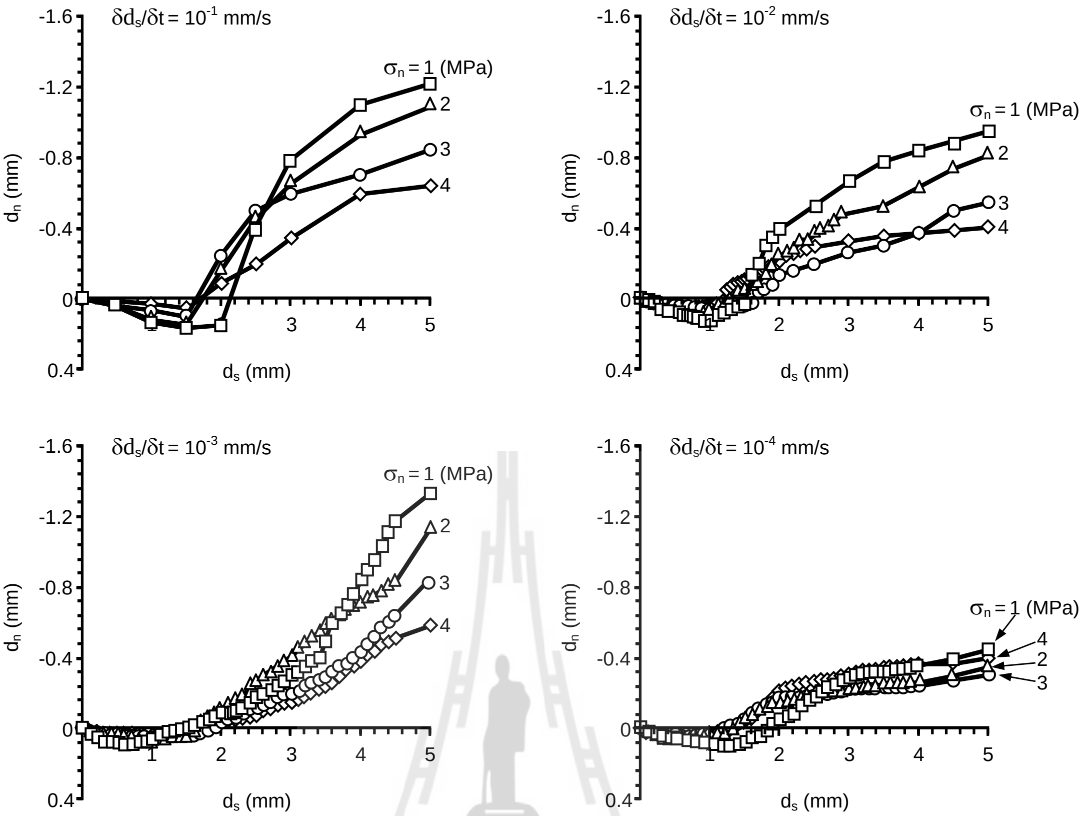

Figure 4.8 Normal displacement (d_n) of PK sandstone as a function of shear displacement (d_s).

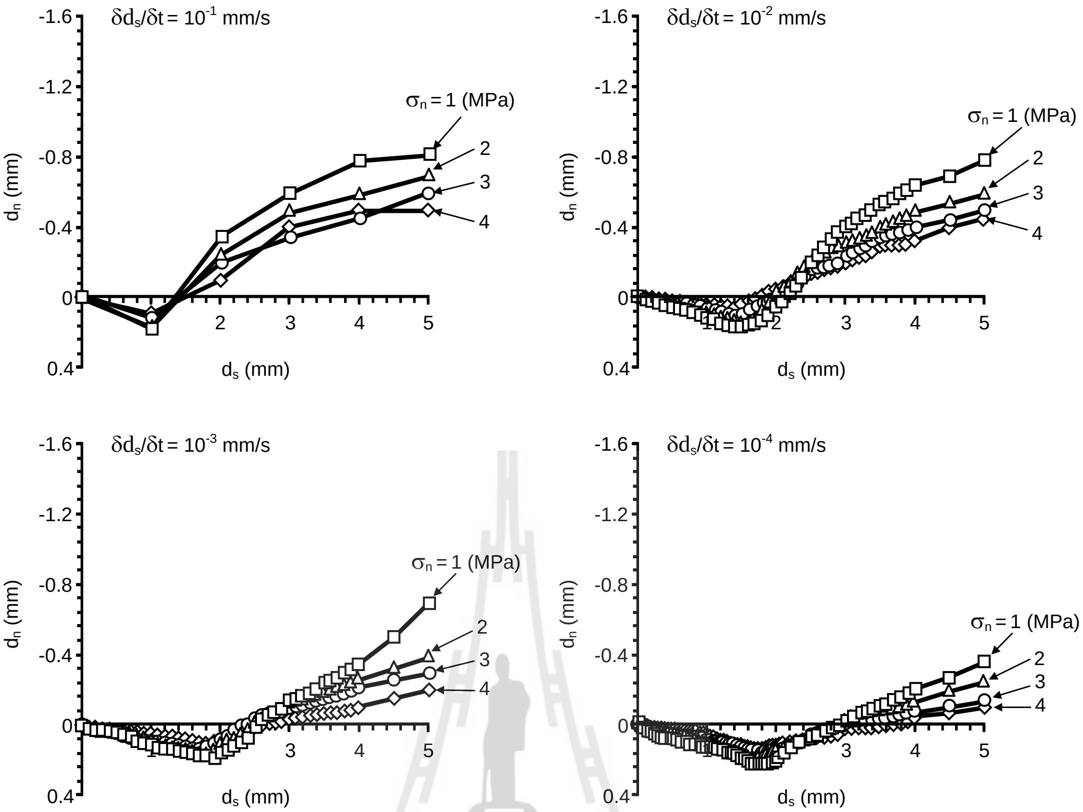

Figure 4.9 Normal displacement (d_n) of PP sandstone as a function of shear displacement (d_s).

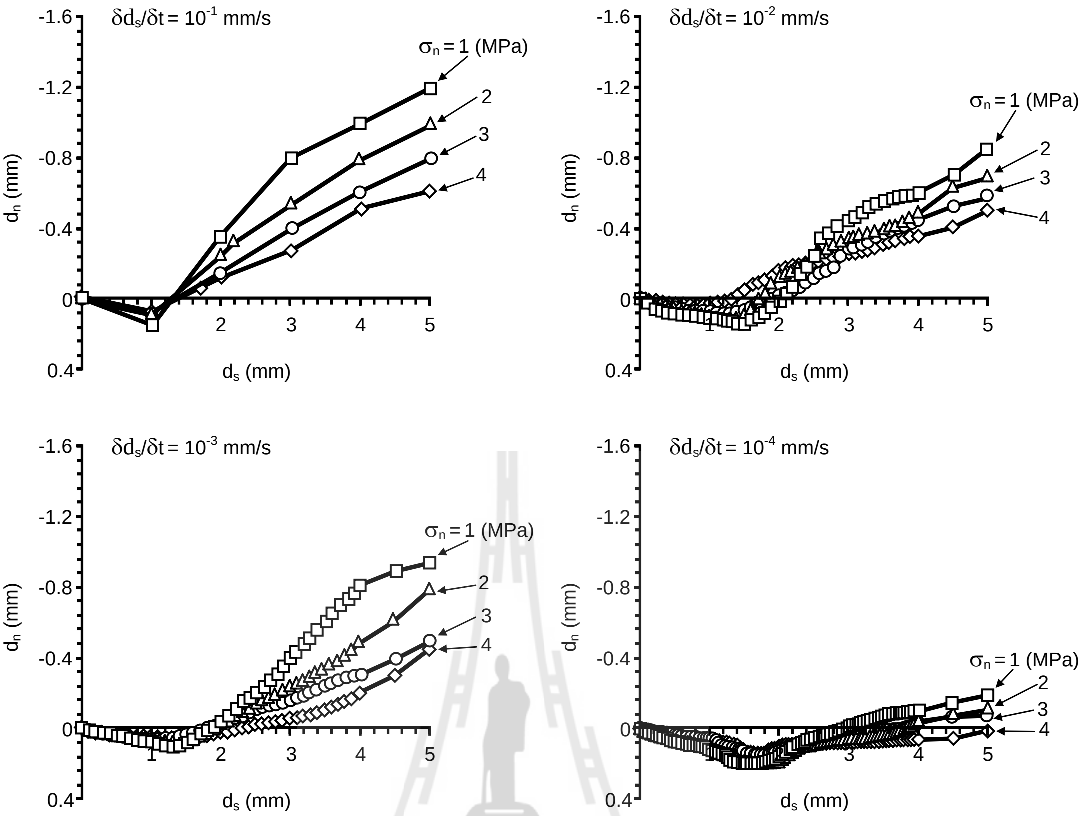

Figure 4.10 Normal displacement (d_n) of PW sandstone as a function of shear displacement (d_s).

Table 4.1 Peak and residual shear strengths for various shear velocities of PK, PP and PW sandstones.

σ_n (MPa)	$\delta d_s/\delta t$ (mm/s)	PK sandstone		PP sandstone		PW sandstone	
		Average JRC = 7		6		12	
		τ_p (MPa)	τ_r (MPa)	τ_p (MPa)	τ_r (MPa)	τ_p (MPa)	τ_r (MPa)
1	10^{-1}	1.97	1.41	1.59	0.94	1.87	0.57
	10^{-2}	1.50	1.12	1.30	0.97	1.69	1.31
	10^{-3}	0.99	0.78	1.08	0.66	1.45	1.31
	10^{-4}	0.81	0.57	0.84	0.71	1.27	1.13
2	10^{-1}	2.57	1.82	2.47	1.63	2.75	1.82
	10^{-2}	2.29	1.63	2.03	1.70	2.38	1.63
	10^{-3}	1.82	1.54	1.87	1.35	1.91	1.45
	10^{-4}	1.44	1.17	1.54	1.26	1.82	1.63
3	10^{-1}	3.55	2.62	3.27	2.90	3.27	2.80
	10^{-2}	3.08	2.34	2.93	2.62	2.99	2.71
	10^{-3}	2.43	2.15	2.52	2.06	2.71	1.96
	10^{-4}	2.08	1.78	2.10	1.87	2.24	1.87
4	10^{-1}	4.13	3.17	3.73	3.27	3.83	3.17
	10^{-2}	3.64	2.89	3.55	3.17	3.55	2.89
	10^{-3}	3.08	2.61	3.03	2.61	3.08	2.33
	10^{-4}	2.80	2.33	2.89	2.52	2.89	2.33

Table 4.2 Joint shear stiffness for various shear velocities and normal stress of PK, PP and PW sandstones.

Rock types	$\delta d_s/\delta t$ (mm/s)	Normal stress, σ_n (MPa)			
		1	2	3	4
PK	10^{-1}	1.10	1.48	1.62	1.90
	10^{-2}	0.95	1.20	1.45	1.70
	10^{-3}	0.75	0.97	1.23	1.45
	10^{-4}	0.67	0.79	1.12	1.30
PP	10^{-1}	0.84	1.07	1.78	1.96
	10^{-2}	0.75	0.93	1.50	1.79
	10^{-3}	0.52	0.70	1.14	1.44
	10^{-4}	0.32	0.62	0.85	1.04
PW	10^{-1}	1.20	1.70	2.10	2.80
	10^{-2}	0.93	1.48	1.80	2.51
	10^{-3}	0.66	1.12	1.45	2.15
	10^{-4}	0.45	0.80	1.03	1.60

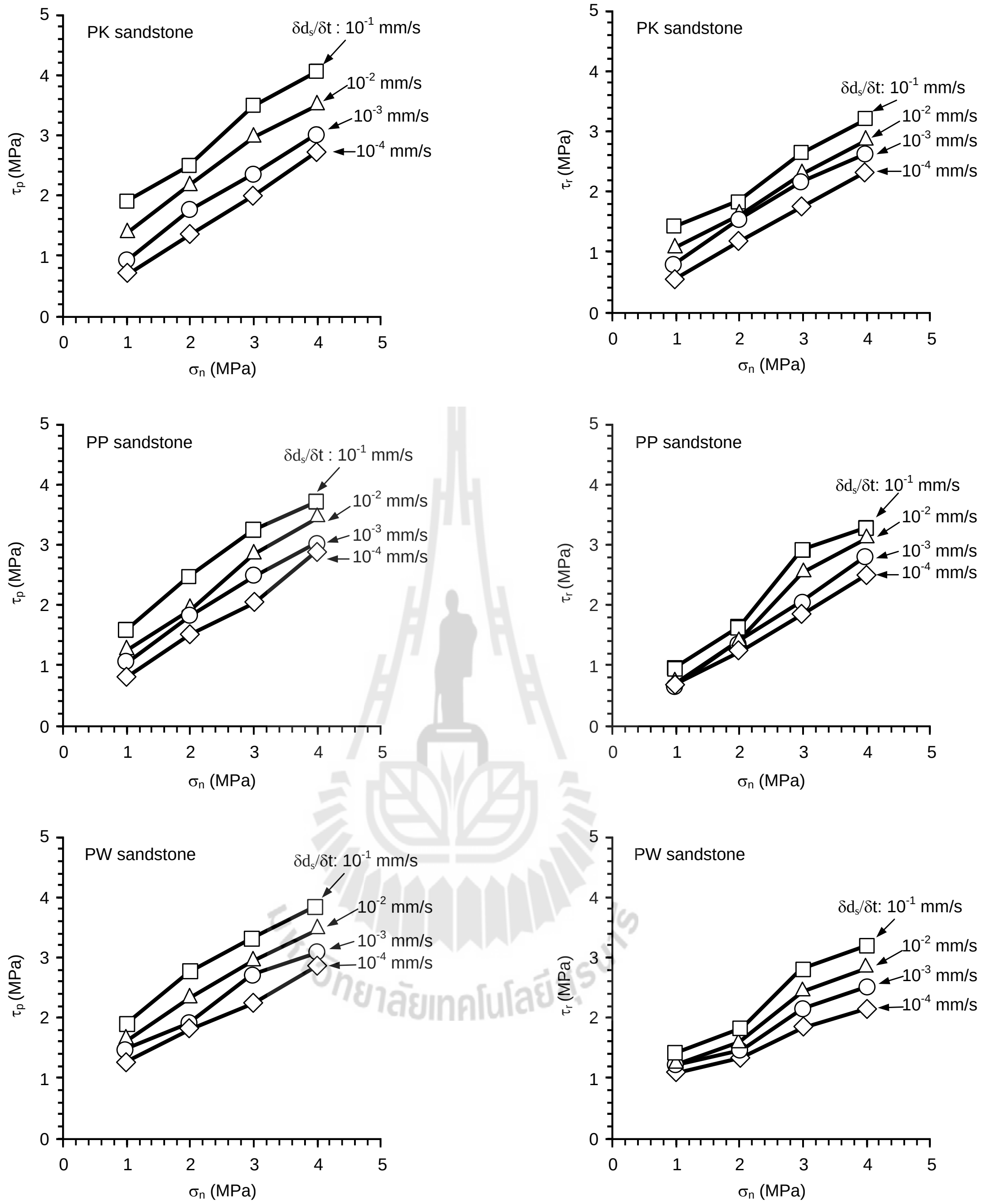

Figure 4.11 Peak and residual shear strengths under various shear velocities ($\delta d_s/\delta t$).

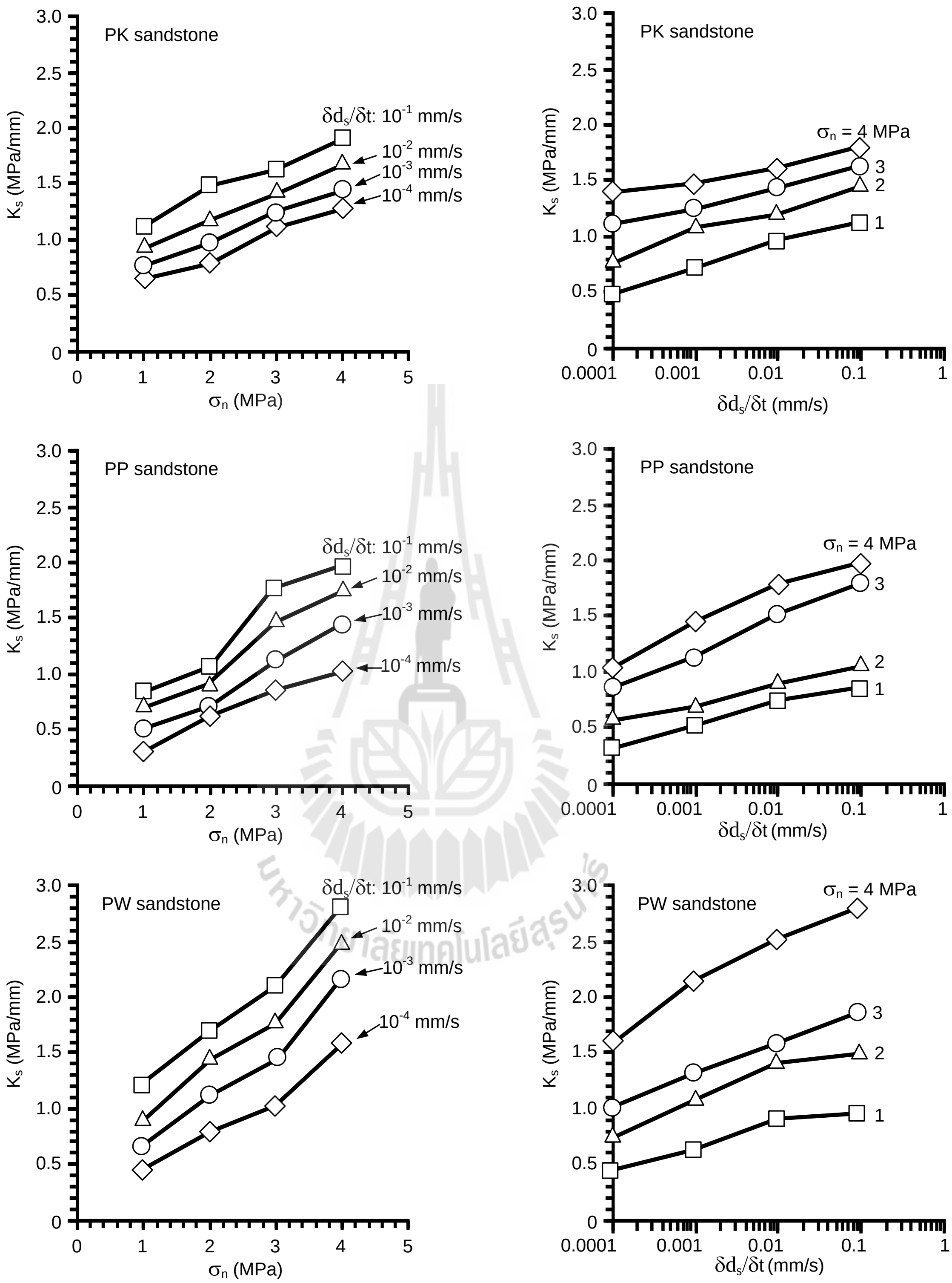

Figure 4.12 Joint shear stiffness as a function of normal stress (σ_n) and shear velocities ($\delta d_s/\delta t$).

CHAPTER V

MATHEMATIC RELATIONS

5.1 Introduction

The objective of this chapter is to develop mathematic equations to describe the effects of shear velocity on fracture shear strengths and stiffness. The Coulomb and Barton criteria are applied to the results.

5.2 Coulomb Criterion

Based on the Coulomb criterion, the shear stress (τ) can be represented by:

$$\tau = c + \sigma_n \tan \phi \tag{5.1}$$

where σ_n is the normal stress, c is the cohesion and ϕ is the friction angle. The cohesion and friction angle of all specimens are summarized in Table 5.1. They can be determined as a function of the shear velocity as follows (Figure 5.1):

$$c = X \cdot \ln(\delta d_s/\delta t) + Y \tag{5.2}$$

$$\phi = I \cdot \ln(\delta d_s/\delta t) + J \tag{5.3}$$

where parameters X, Y, I and J are empirical constants as shown in Table 5.2.Substituting equations (5.2) and (5.3) into (5.1), the shear strength (τ) can be written as:

$$\tau = [\ X \cdot \ln(\delta d_s/\delta t) + Y\ ] + \sigma_n \tan [\ I \cdot \ln(\delta d_s/\delta t) + J\ ] \tag{5.4}$$

Figure 5.2 shows the compared peak shear strength under various shear velocities based on Coulomb derived equation and result tested. The result is fit similar.

Table 5.1 Cohesion and friction angle for various shear velocities of PK, PP and PW sandstones.

Type	$\delta d_s/\delta t$ (mm/s)	JRC (average)	c (MPa)	ϕ (Degrees)	R^2
PK	10^{-1}	7	1.18	37	0.989
	10^{-2}		0.83	37	0.993
	10^{-3}		0.37	35	0.995
	10^{-4}		0.13	35	0.999
PP	10^{-1}	6	0.96	36	0.982
	10^{-2}		0.54	37	0.995
	10^{-3}		0.50	33	0.991
	10^{-4}		0.16	34	0.996
PW	10^{-1}	12	1.34	33	0.983
	10^{-2}		1.10	32	0.997
	10^{-3}		0.87	30	0.981
	10^{-4}		0.73	28	0.993

Table 5.2 Constants X, Y, J, and K for all tested rocks.

Rock type	X	Y	I	J
PK	0.16	1.53	0.35	38.0
PP	0.11	1.15	0.43	37.5
PW	0.09	1.53	0.74	35.0

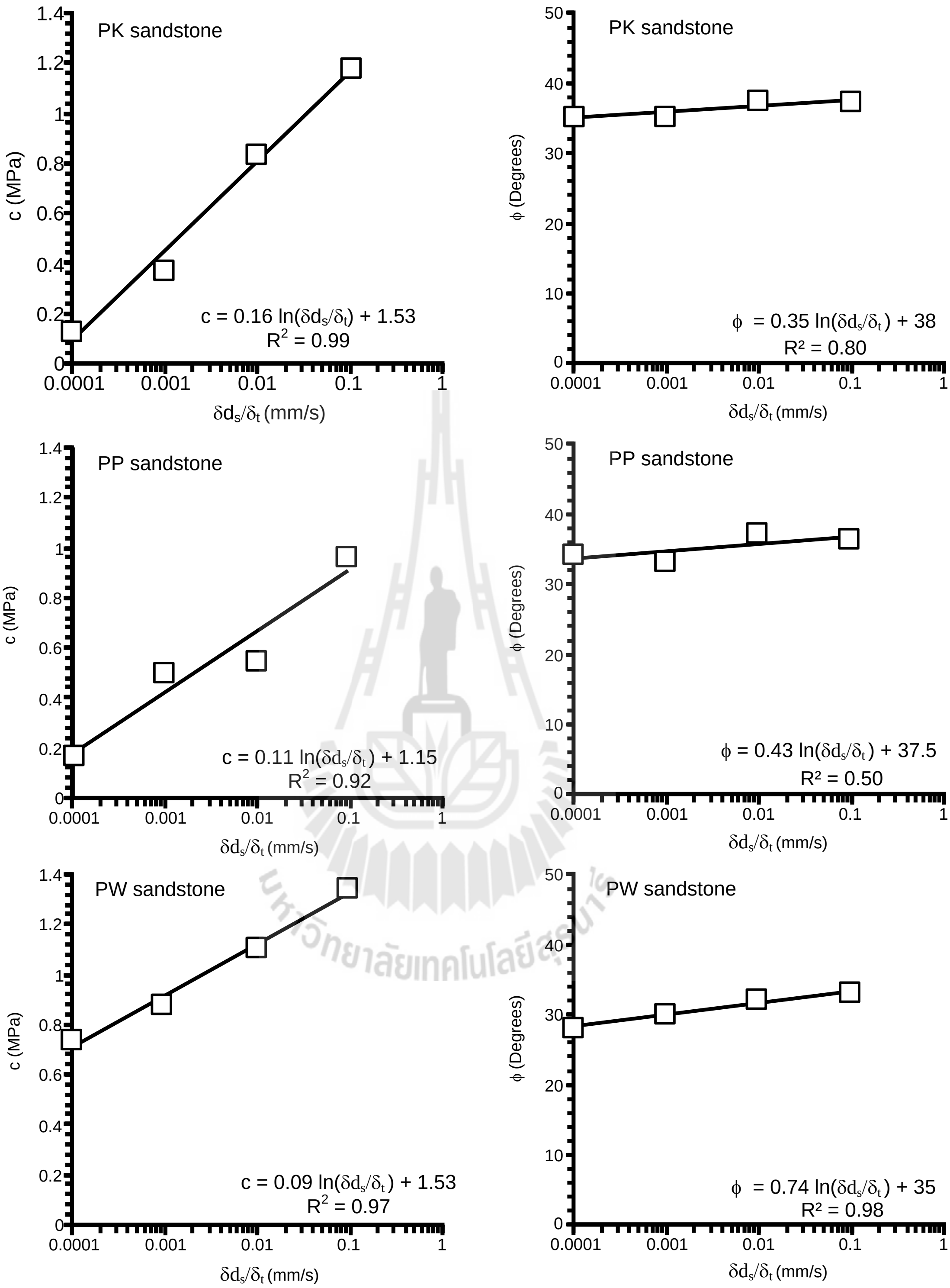

Figure 5.1 Cohesion (c) and friction angle (ϕ) of PK, PP and PW sandstones as a function of the shear velocity ($\delta d_s/\delta t$).

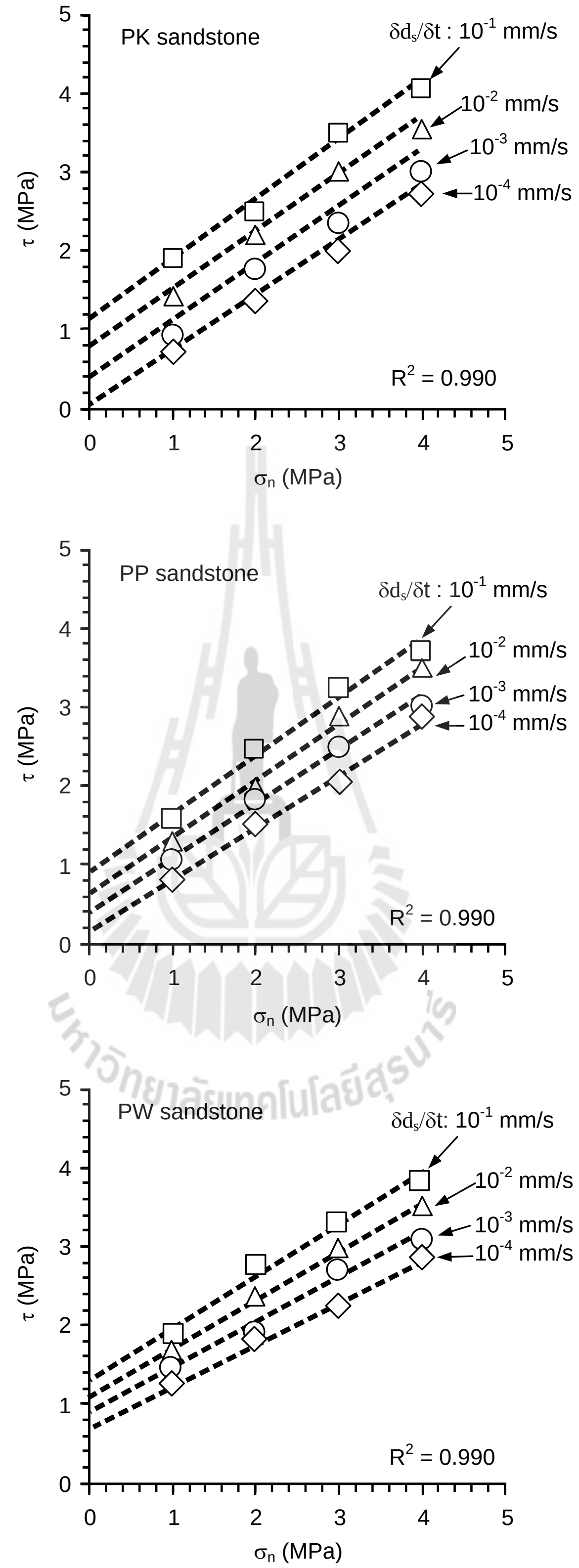

Figure 5.2 The comparison of peak shear strength base on coulomb derived equation (dash line) and result tested (symbol).

5.3 Barton Criterion

The Barton criterion can be defined as:

$$\tau = \sigma_n \tan\left(\phi_b + \text{JRC}\log_{10}\left(\frac{\text{JCS}}{\sigma_n}\right)\right) \tag{5.5}$$

where σ_n is the normal stress, JRC is the joint roughness coefficient, ϕ_b is the basic friction angle, and JCS is joint compressive strength. The average JRC and basic friction angle of all rock types are summarized in Tables 5.3. The JCS can solve back from equation 5.6.

$$\text{JCS} = \sigma_n 10^{\left\{\frac{\tan^{-1}\left[\frac{\tau}{\sigma_n}\right]-\phi_b}{\text{JRC}}\right\}} \tag{5.6}$$

Table 5.4 shows the value of average JCS. Then values can be determined as a function of the shear velocity as follows (Figure 5.3):

$$\text{JCS} = \text{M}(\delta d_s/\delta t)^{\text{N}} \tag{5.7}$$

where parameters M and N are empirical constants as shown in Table 5.5.

Substituting equations (5.7) into (5.5), the shear strength (τ) can be written as:

$$\tau = \sigma_n \tan\left(\phi_b + \text{JRC}\log_{10}\left(\frac{\text{M}(\delta d_s / \delta t)^N}{\sigma_n}\right)\right) \tag{5.8}$$

Figure 5.4 shows the compared peak shear strength under various shear velocities based on Barton derived equation and result tested.

Table 5.3 Joint roughness coefficient and basic friction angles of PK, PP and PW sandstones

Rock types	JRC (average)	ϕ_b (Degrees)
PK	7	33
PP	6	31
PW	12	31

Table 5.4 Joint compressive strength for various velocities of PK, PP and PW sandstones.

$\delta d_s/\delta t$ (mm/s)	Joint compressive strength (JCS)		
	PK	PP	PW
10^{-1}	1683.17	1255.94	84.20
10^{-2}	202.36	315.48	42.20
10^{-3}	24.33	79.24	21.15
10^{-4}	2.93	19.91	10.60

Table 5.5 Constants M and N for all rock types.

Rock types	M	N
PK	14000	0.92
PP	5000	0.6
PW	168	0.3

5.4 Joint Shear Stiffness

Joint shear stiffness (K_s) is calculated from the linear slope of the shear stress-displacement curves ($\delta d_s/\delta t$). The shear stiffness tends to increase linearly with increasing the normal stress, which can be represented by:

$$K_s = \omega \cdot \sigma_n + A \tag{5.9}$$

where ω and A are empirical constants depending on the shear velocities applied. Figure 5.5 shows the parameters ω and A of the PW, PK and PP sandstones as a function of the shear velocities ($\delta d_s/\delta t$). They can be represented by the following relations:

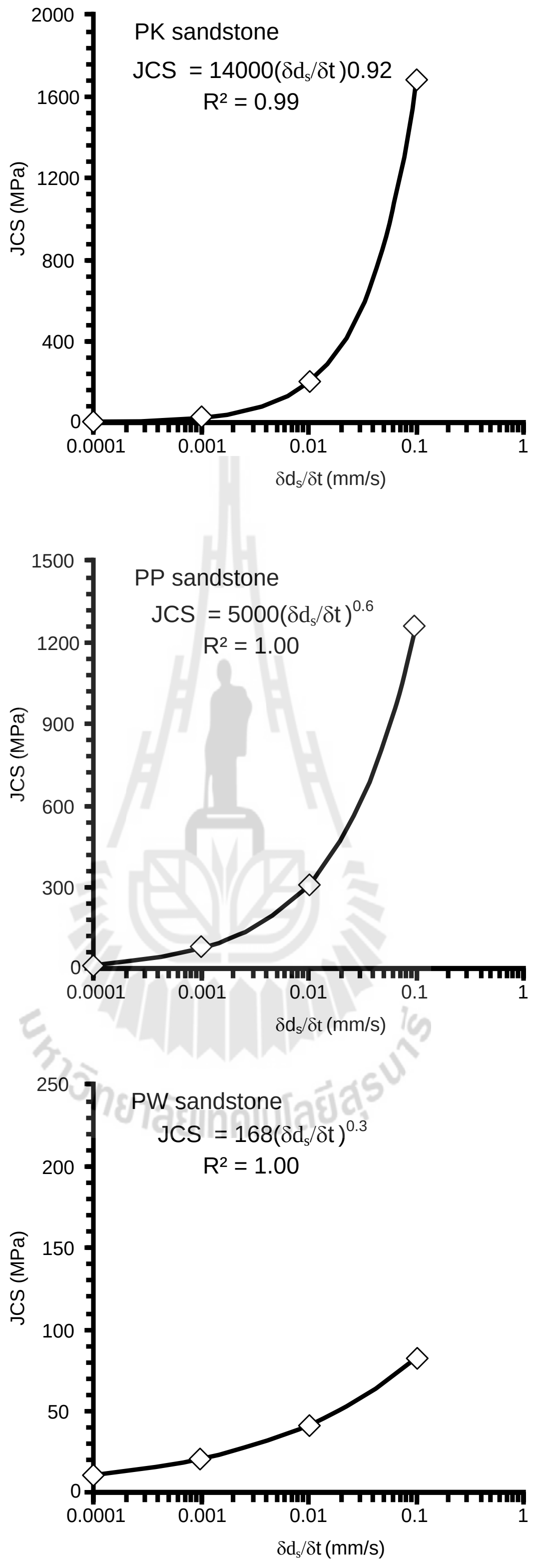

Figure 5.3 Joint compressive strength (JCS) of PK, PP and PW sandstones as a function of the shear velocities ($\delta d_s/\delta t$).

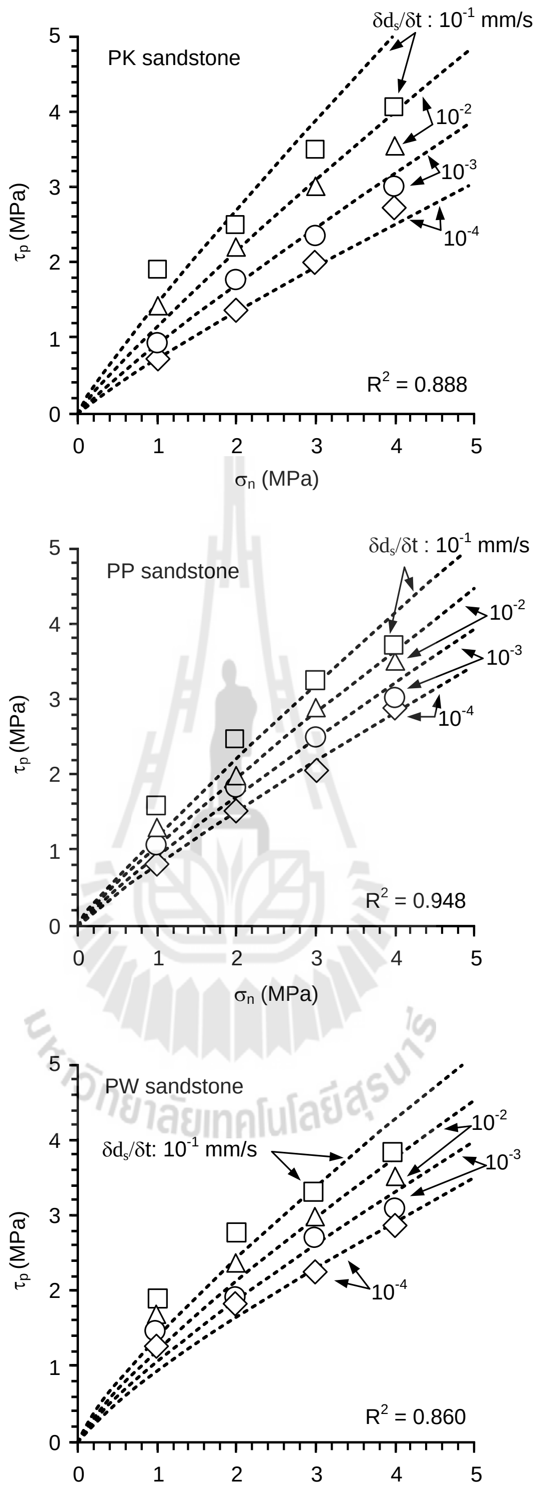

Figure 5.4 Peak shear strength under various velocities based on Barton derived equation and result tested.

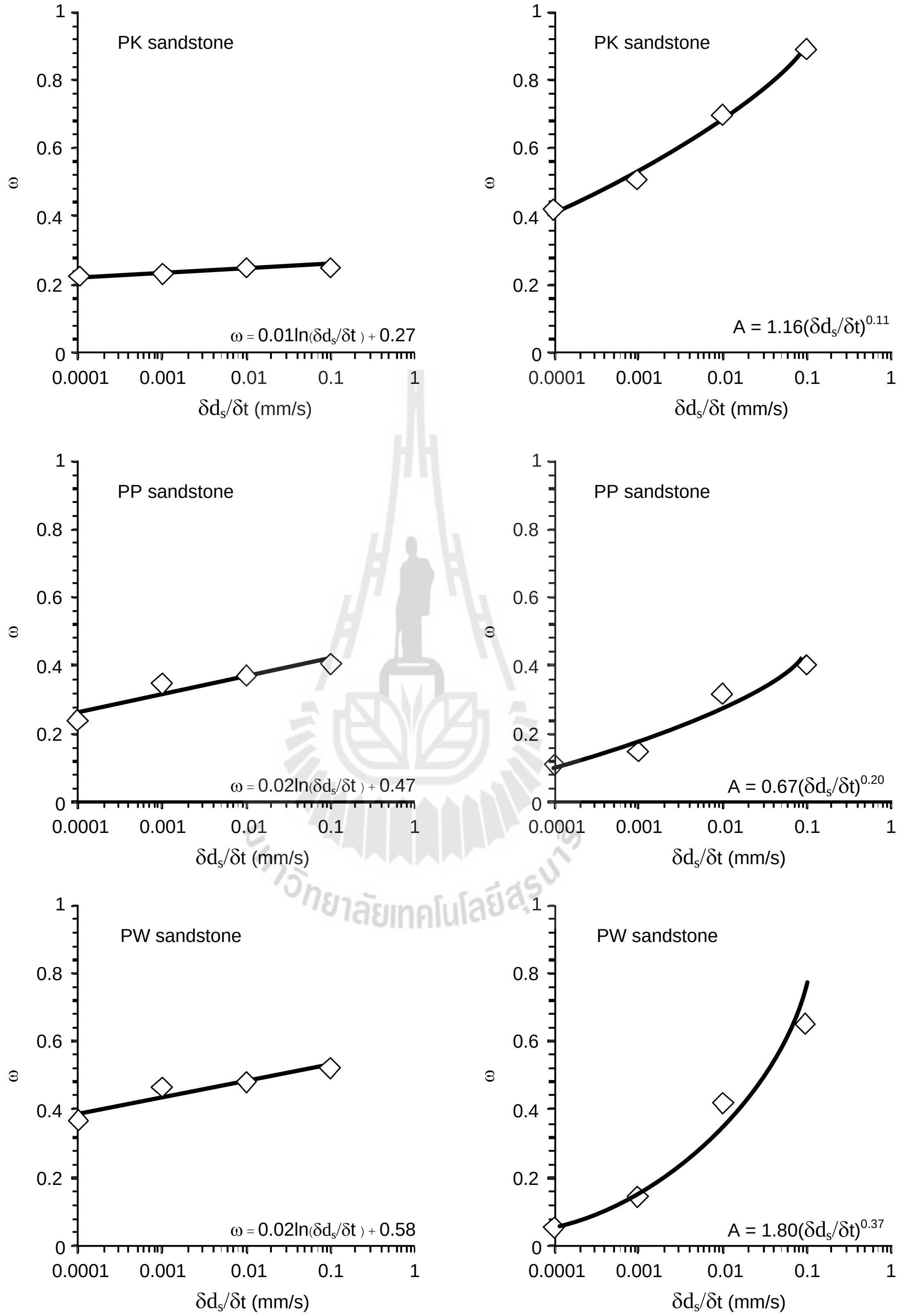

Figure 5.5 Parameters ω and A as a function of shear velocities ($\delta d_s/\delta t$).

$$\omega = \alpha \cdot \ln(\delta d_s / \delta t) + L \tag{5.10}$$

$$A = \beta \cdot (\delta d_s / \delta t)^{\kappa} \tag{5.11}$$

The parameters α, L, β and κ are empirical constants as shown in Table 5.6. Substituting equations (5.10) and (5.11) into (5.9) the joint shear stiffness (K_s) can be written as:

$$K_s = [\alpha \cdot \ln(\delta d_s / \delta t) + L] \cdot \sigma n + [\beta \cdot (\delta d_s / \delta t)^{\kappa}] \tag{5.12}$$

Figure 5.6 The comparison between joint shear stiffness from derived equation and result tested. The result fit similar.

Table 5.6 Constant α, L, β and κ for all rock types.

Rock types	α	L	β	κ
PK	0.01	0.27	1.16	0.11
PP	0.02	0.47	0.67	0.20
PW	0.02	0.58	1.80	0.37

5.5 Dilation

Table 5.7 lists the slopes of the normal displacement and shear displacement curve (dilation) for all specimens. The higher velocity is applied, the higher dilation is obtained, as shown in Figure 5.7. However, the higher normal stress applied, the lower dilation is obtained as shown in Figure 5.8.

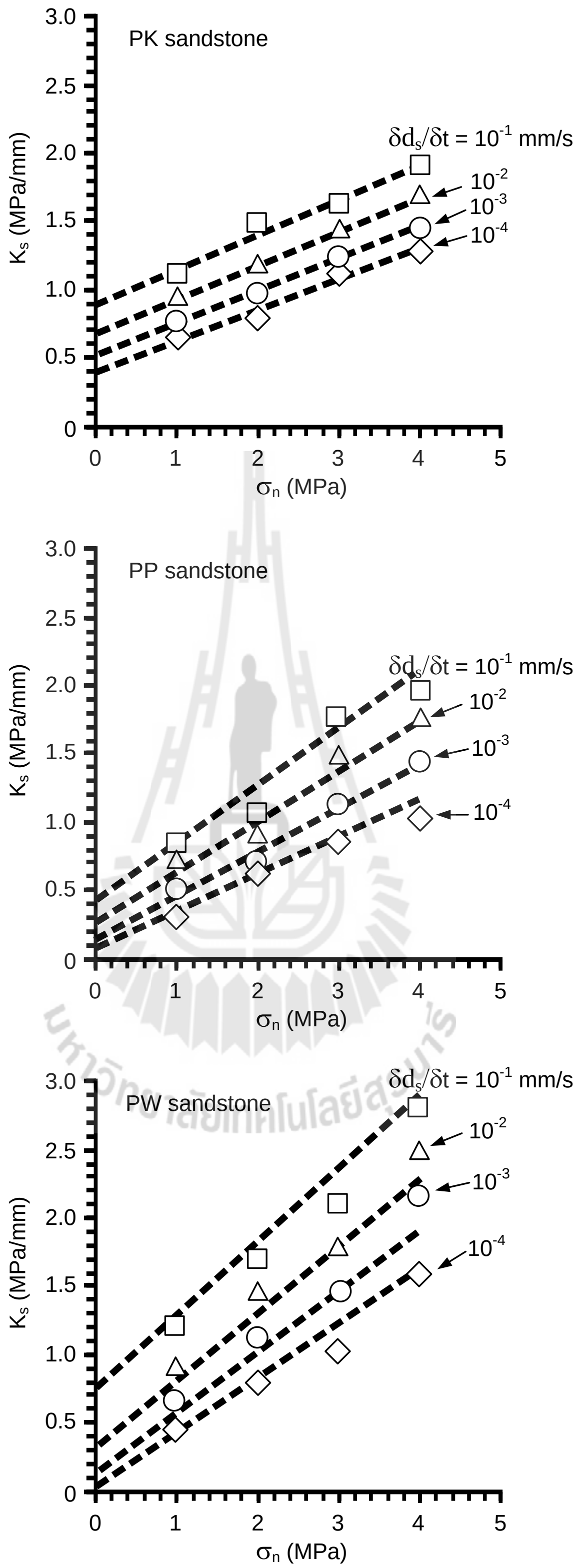

Figure 5.6 The comparison joint shear stiffness on derived equation (dash line) and result tested (symbol).

Table 5.7 Dilation of PK, PP and PW sandstones.

Rock types	$\delta d_s/\delta t$ (mm/s)	Normal stress (MPa)			
		1	2	3	4
PK	10^{-1}	0.70	0.58	0.43	0.32
	10^{-2}	0.59	0.47	0.38	0.29
	10^{-3}	0.47	0.39	0.31	0.19
	10^{-4}	0.41	0.30	0.24	0.16
PP	10^{-1}	0.53	0.41	0.32	0.19
	10^{-2}	0.37	0.33	0.22	0.16
	10^{-3}	0.26	0.20	0.15	0.11
	10^{-4}	0.21	0.16	0.12	0.08
PW	10^{-1}	0.34	0.30	0.22	0.15
	10^{-2}	0.31	0.25	0.19	0.12
	10^{-3}	0.27	0.18	0.14	0.09
	10^{-4}	0.21	0.13	0.05	0.04

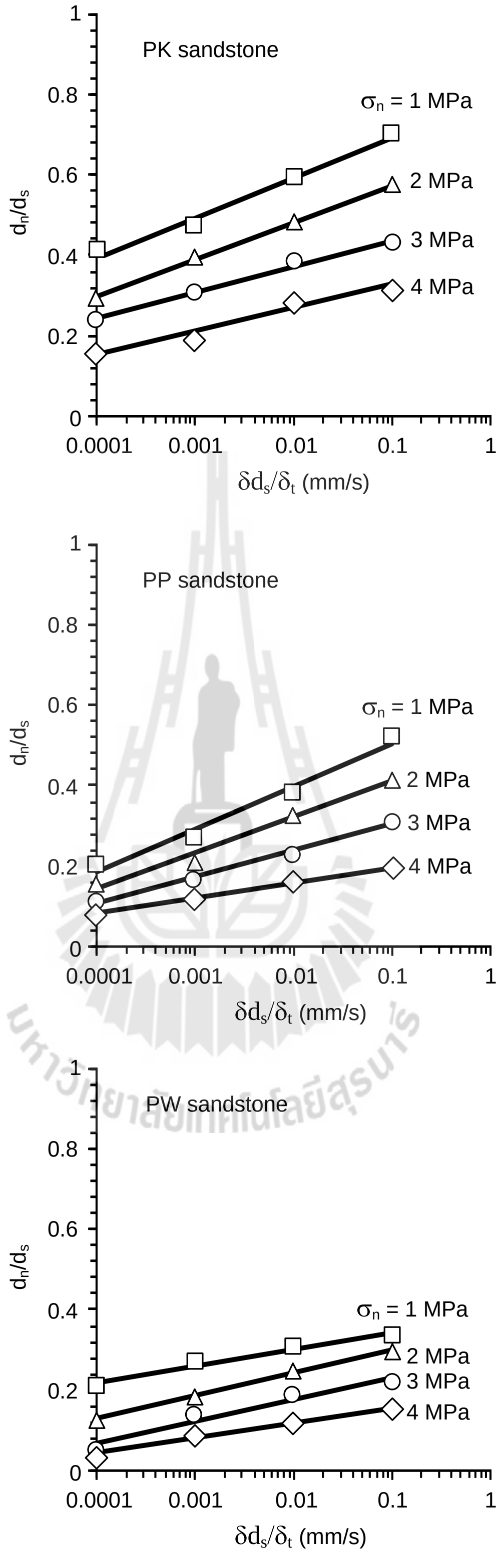

Figure 5.7 Dilation of PK, PP and PW sandstone fractures as a function of the shear velocities ($\delta d_s/\delta t$).

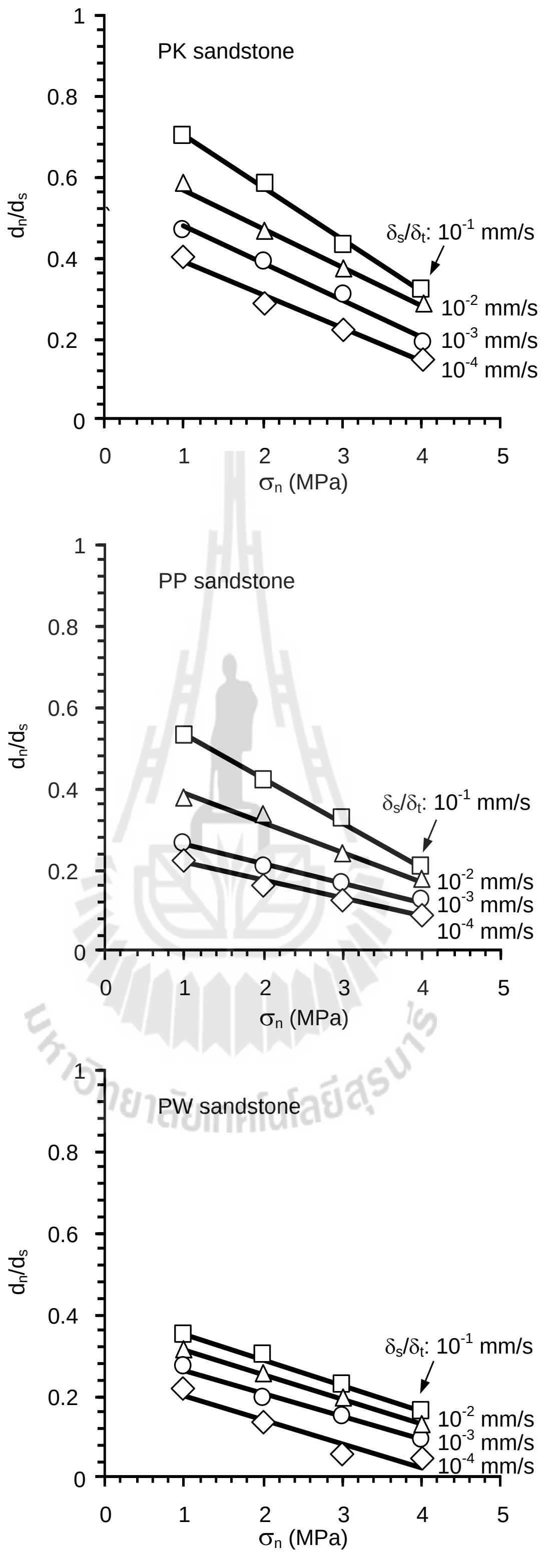

Figure 5.8 Dilation of PK, PP and PW sandstone fractures as a function of normal stress (σ_n).

CHAPTER VI

DISCUSSIONS OF THE RESULTS

The shear velocities can affect the shear strengths of the tension-induced fractures in the PP, PW and PK sandstones. Here the Coulomb's criterion can well describe the joint shear strengths of the rocks under the shear velocities ranging from 10^{-4} to 10^{-1} mm/s with the normal stresses from 1 to 4 MPa. The higher shear velocities applied, the higher the peak and residual shear stresses are obtained particularly under high normal stresses. Since the JRC values for all specimens of each sandstones type are in a narrow range (6 to 12) it is assumed that the roughness of the intension-induced fractures is the same for each sandstone type. As a result the cohesion and friction angle obtained for the Coulomb criterion can be correlated among different shear velocities. It is found that both cohesion and friction angle notably increase with the shear velocities. The cohesion can be as low as zero under the shear velocities of 10^{-4} mm/s to about 0.3-0.5 MPa under the shear velocities of 10^{-1} mm/s. The friction angles can increase by about 2-5 degrees when the shear velocities increase from 10^{-4} to 10^{-1} mm/s. The slope of normal and shear displacement curve (dilation) are higher when higher velocity and the higher normal stress, the lower dilation obtain. The scattering of the data is probably due to the intrinsic variability of the tested fracture.

The shear strengths are clearly independent of the shear velocities. This suggests that the rate-dependent shear strength and stiffness of the tension-induced fractures is primarily due to the time-dependent strength of the rock asperities on the fracture wall. This supported by the experimental results obtained by Fuenkajorn and Khenkhunthod (2010) who conclude that the uniaxial and triaxial compressive strengths and elastic modulus of the three sandstones increase exponentially with the loading rate. It can therefore be postulated that the time-dependent shear strengths of the fractures may be found in other rock types of which compressive strengths are sensitive to loading rate. The comparison of **Table 6.1** and **Table 6.2** shows the time-dependent shear strength that relates to the rock strength.

Table 6.1 Compressive strength PW of Fuenkajorn and Khenkhunthod (2010).

$\delta\sigma_1/\delta t$ (MPa/s)	Compressive strength, σ_c (MPa)			
	Confining stress = 0 MPa	3 MPa	7 MPa	12 MPa
10	83.50	110	130	145
1.0	68.60	102	121.67	146.62
0.1	64.62	85.50	109.26	143.94
0.01	57.80	80.16	95.48	135.04
0.001	46.80	73.64	90.6	130.20

Table 6.2 Shear strength PW of this study.

$\delta d_s/\delta t$ (mm/s)	Shear strength, τ_{peak} (MPa)			
	Normal stress = 1 MPa	2 MPa	3 MPa	4 MPa
0.1	1.87	2.75	3.27	3.83
0.01	1.69	2.38	2.99	3.55
0.001	1.45	1.91	2.71	3.08
0.0001	1.27	1.82	2.24	2.89

The result of this study agree with the study on time-dependent rock strength by Sang and Dhir (1972) who investigate the influence of strain rate on the strength, deformation and fracture properties of Lower Devonian sandstone. Comparison of strength results obtained at different loading and rates showed that for similar loading times to failure the constant rates of loading give slightly higher strength values. This agrees with the observation by Ray et al. (1999). A clear increase in uniaxial compressive strength is observed with increase in strain rate. Stress is found to increase with the increase in strain rate and Young's modulus was found to increase with the increase in strain rate. However, this study disagrees with the result by Jafari et al. (2003), who study the effects of displacement rates (or shearing velocity) on shear strength. It is observed that shear strength reduces with increasing shears velocity, approaching the same values for the peak and residual strength at higher shearing velocities. They study on smaller range of shear velocities, while this study has large range of shear velocities.

CHAPTER VII

CONCLUSIONS AND RECOMMENDATIONS FOR FUTURE STUDIES

7.1 Conclusions

This study is aimed to experimentally assess effect of shear velocities on joint shear strength and joint stiffness of fracture sandstones. In this study the Coulomb and Barton criteria are used. The results indicate that the low shear velocities decrease the peak and residual shear strengths, including cohesion and friction angle based on Coulomb criteria. Joint shear stiffness increases with shear velocities. All parameters tend to increase linearly with normal stress and shear velocities. Joint compressive strength tends to increase exponential with shear velocities as a result the Barton criterion overestimates the test result. The comparison of the Coulomb and Barton criteria are different before and after of peak shear strength curve. The dilation are change with shear velocities. The dilation rates increase with the shear velocities.

7.2 Recommendations for future studies

More rock samples should be tested under a wider range of normal stresses. Different shear velocities may be applied. The results will be very useful to construct a generally empirical rock to quantitatively determine the effect of shear velocities on the friction of rock joints. It is also desirable to correlate the scale and time-dependent effects on the intact rock strength with the rate-dependent shear strength of the joints.

REFERENCES

Barton, N. (1973). Review of a new shear-strength criterion for rock joints. **Engineering Geology**. 7(4): 287-332.

Crawford, A. M. and Curran, J. H. (1981). The influence of shear velocity on the frictional resistance of rock discontinuities. **International Journal of Rock Mechanics and Mining Sciences & Geomechanics.** 18(6): 505-515.

Fuenkajorn, K. and Kenkhunthod, N. (2010). Influence of loading rate on deformability and compressive strength of three Thai sandstone. **Geotechnical and Geological Engineering**. 28(5): 707-715.

Jafari, M.K., Hosseini, K. A., Boulon, M., Pellet, F., Jalaly, H., Uromeihy, A. and Buzzy, O. (2002). Laboratory investigation on shear strength variation of joint replicas due to low and high amplitude cyclic displacements. **Journal of Seismology and Earthquake Engineering** 4 (2-3): 37-49.

Jafari, M.K., Hosseini, K.A., Pellet, F., Boulon, M. and Buzzi, O. (2003). Evaluation of shear strength of rock joints subjected to cyclic loading. **Soil Dynamics and Earthquake Engineering** 23 (7): 619-630.

Kemeny, J. (2003). The Time-Dependent Reduction of Sliding Cohesion due to Rock Bridges Along Discontinuities: A Fracture Mechanics Approach. **Rock Mechanics and Rock Engineering** 36 (1): 27-38.

Kemthong, R. and Fuenkajorn, K. (2007). Prediction of joint shear strengths of ten rock types using field-identified parameters. **Proceedings of the First Thailand Symposium on Rock Mechanics**, Khao Yai, Thailand, Geomechanics Research Unit, Institute of Engineering Suranaree University of Technology, Thailand pp.195-209.

Kenkhunthod, N. and Fuenkajorn, K. (2010). Influence of loading rate on deformability and compressive strength of three Thai sandstones. **Geotechnical and Geological Engineering** 28(5): 707-715.

Kwafniewskil; M.A. and Wang, J.A. (1997). Surface roughness evolution and mechanical behavior of rock joints under shear. **International Journal of Rock Mechanics & Mining Sciences** 34 (3-4): 157.e1-157.e14.

Lee, H.S., Park, Y.J., Cho, T.F. and You, K.H. (2001). Influence of asperity degradation on the mechanical behavior of rough rock joints under cyclic shear loading. **International Journal of Rock Mechanics & Mining Sciences** 38 (7): 967-980.

Ma, L. and Daemen, J. J. K. (2006). Strain rate dependent strength and stress-strain characteristics of a welded tuff. **Bulletin of Engineering Geology and the Environment** 65(3): 221-230.

Park, J.W. and Song, J.J. (2009). Numerical simulation of a direct shear test on a rock joint using a bonded-particle model. **International Journal of Rock Mechanics & Mining Sciences** 46 (8): 1315-1328.

Ray, S. K., Srakar, M. and Singh, T. N. (1999). Effect of cyclic loading and strain rate on the mechanical behaviour of sandstone. **International Journal of Rock Mechanics and Mining Sciences** 36: 543-549.

Sangha, C. M. and Dhir, R. K. (1972). Influence of time on the strength, deformation and fracture properties of a lower Devonian sandstone. **International Journal of Rock Mechanics and Mining Sciences** 9: 343-354.

Seidel, J.P. and Haberfield, C.M. (2002). A Theoretical Model For Rock Joints Subjected To Constant Normal Stiffness Direct Shear. **International Journal of Rock Mechanics and Mining Sciences** 39 (5): 539-553.

Vasarhelyi, B. (1998). Influence of normal load on joint dilatation rate. **Rock Mechanics and Rock Engineering** 31 (2): 117-123.

BIOGRAPHY

Mr. Hasun Kodae was born on March 3, 1989 in Naratiwat province, Thailand. He received his Bachelor's Degree in Engineering (Geotechnology) from Suranaree University of Technology in 2010. For him post-graduate, he continued to study with a Master's degree in the Geological Engineering Program, Institute of Engineering, Suranaree University of Technology.